ACS OMEGA

Open Access

http://pubs.acs.org/journal/acsodf

Article

New Chalcogen-Functionalized Naphthoquinones: Design, Synthesis, and Evaluation, *In Vitro* and *In Silico*, against Squamous Cell Carcinoma

Luana da Silva Gomes, Érica de Oliveira Costa, Thuany G. Duarte, Thiago S. Charret, Raquel C. Castiglione, Rafael L. Simões, Vinicius D. B. Pascoal, Thiago H. Döring, Fernando de C. da Silva, Vitor F. Ferreira, Aldo S. de Oliveira, Aislan C. R. F. Pascoal, André L. S. Cruz, and Vanessa Nascimento*

Cite This: *ACS Omega* 2024, 9, 21948−21963

Read Online

ACCESS | Metrics & More | Article Recommendations | Supporting Information

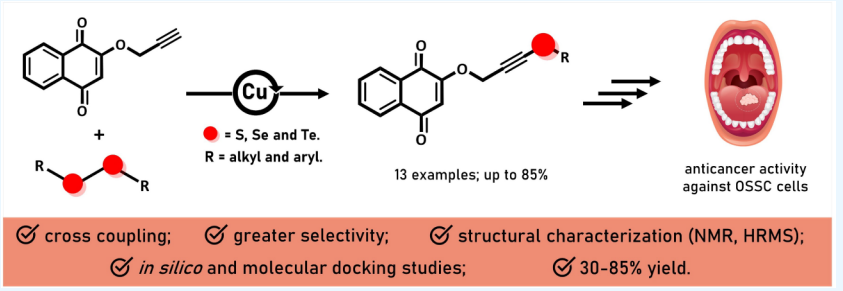

ABSTRACT: Due to the growth in the number of patients and the complexity involved in anticancer therapies, new therapeutic approaches are urgent and necessary. In this context, compounds containing the selenium atom can be employed in developing new medicines due to their potential therapeutic efficacy and unique modes of action. Furthermore, tellurium, a previously unknown element, has emerged as a promising possibility in chalcogen-containing compounds. In this study, 13 target compounds (**9a−i**, **10a−c**, and **11**) were effectively synthesized as potential anticancer agents, employing a CuI-catalyzed Csp-chalcogen bond formation procedure. The developed methodology yielded excellent results, ranging from 30 to 85%, and the compounds were carefully characterized. Eight of these compounds showed promise as potential therapeutic drugs due to their high yields and remarkable selectivity against SCC-9 cells (squamous cell carcinoma). Compound **10a**, in particular, demonstrated exceptional selectivity, making it an excellent choice for cancer cell targeting while sparing healthy cells. Furthermore, complementing *in silico* and molecular docking studies shed light on their physical features and putative modes of action. This research highlights the potential of these compounds in anticancer treatments and lays the way for future drug development efforts.

1. INTRODUCTION

The majority of head and neck cancers originates in squamous cells lining the moist surfaces of the region. This includes tumors affecting the lips, oral cavity, pharynx, larynx, and nasal cavity. Oral squamous cell carcinoma (OSCC), the sixth most common malignant tumor in humans, accounts for about 2% of all cancer cases. Squamous cell carcinomas account for 90% of all oral carcinomas, and approximately 350,000 new cases of oral carcinoma are diagnosed globally each year, resulting in up to 170,000 annual mortalities.[1,2]

Usually, OSCC shows no symptoms in its initial phase, which can be confused with small sores and thrush in the oral cavity. Men are most affected by this pathology, and the risk factors are mainly related to tobacco and alcohol, but in recent years, there have been studies on the influence of persistent human papillomavirus (HPV) infections and Epstein−Barr virus (EBV) in carcinogenesis.[3,4] In addition to these risk factors, we still do not know the possible impact of the use of electronic cigarettes and vaping devices on oral cancer since these products have been marketed aggressively over the past decade as a "safe" alternative to cigarettes.[5]

Chemotherapy is an important part of OSCC treatment and is frequently used in conjunction with radiotherapy and surgery. Unfortunately, the establishment of multidrug resistance mechanisms in specific cell types has been frighteningly rapid, resulting in treatment failures. In the face

Received: December 18, 2023
Revised: April 24, 2024
Accepted: April 29, 2024
Published: May 8, 2024

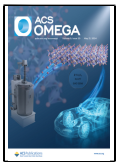

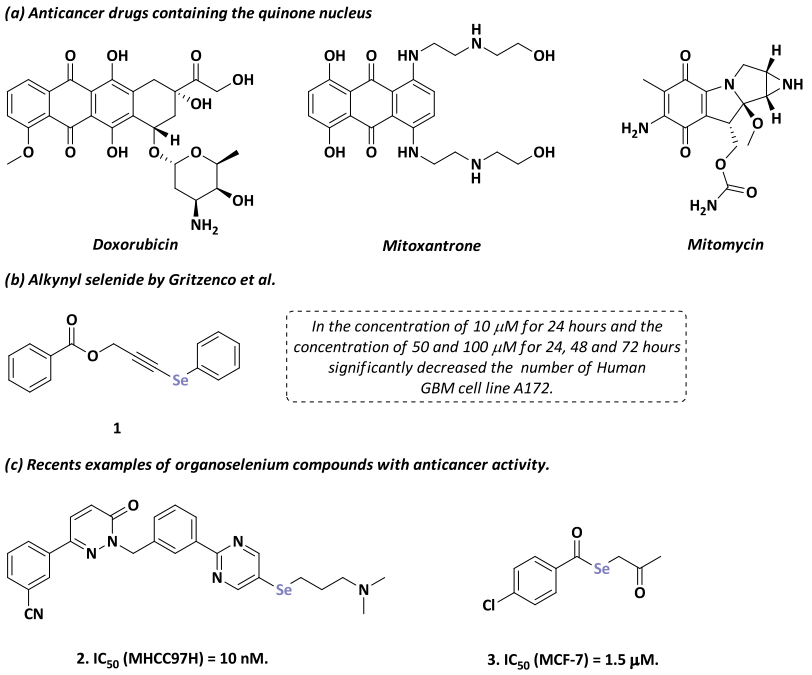

Figure 1. (a) Anticancer drugs containing the quinone nucleus; (b) alkynyl selenide with anticancer activity; (c) recent examples of organoselenium compounds with anticancer activity.

Scheme 1. General Synthetic Route of Alkynyl-Chalcogen-Naphthoquinone Hybrids 9a−i, 10a−c, and 11

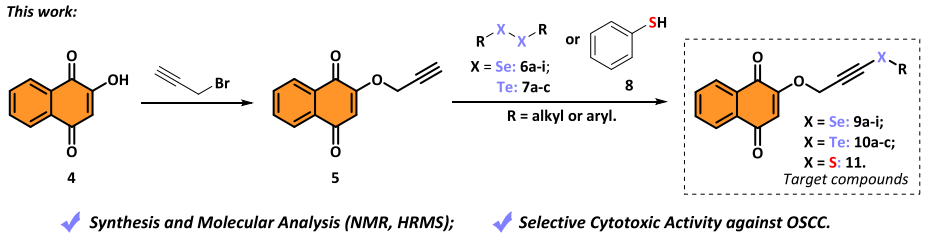

of this escalating crisis, it is becoming increasingly urgent to begin the study and develop new compounds with strong anticancer potential. These compounds have the potential to act as prospective pharmacological agents in the never-ending combat against OSCC, a cancer with troubling data trends indicating a proneness toward worsening outcomes.[6,7]

Naphthoquinones, naturally occurring substances, show numerous biological activities such as antimicrobial,[8] antibacterial,[9] antioxidant,[10] cytotoxic,[11] and antiviral properties,[12] among others.[13] These compounds are closely related to various biochemical processes and biological activities within cells, especially through their participation in the redox cycle. This cycle includes anions, dianions, superoxide anions, and semiquinone radicals, all of which are essential in the formation of reactive oxygen species such as hydrogen peroxide (H_2O_2), superoxide radical anion ($O_2^{-\bullet}$), and hydroxyl radical ($HO^{\bullet}$). In turn, these reactive oxygen species have the potential to harm vital cell components. It is also worth noting that, in relation to chemotherapy, there appears to be an antagonism in the activity of naphthoquinones, which cause cell apoptosis (cell death) in cancer cells that have abnormal proliferation.[14]

For example, doxorubicin, mitoxantrone, and mitomycin are three anticancer drugs that share a common quinone nucleus and continue to hold immense significance in current cancer treatment strategies (Figure 1a). These compounds have demonstrated their mettle across various cancer types, significantly improving patient outcomes. Doxorubicin, renowned for its versatility, tackles a wide range of cancers, while mitoxantrone shines in treating leukemia and prostate cancer. On the other hand, mitomycin's potency extends to colorectal and gastric cancers. These drugs operate by interfering with DNA replication, disrupting the growth of cancer cells, and thus occupy pivotal roles in modern oncology. Their enduring relevance underscores the indispensable role of quinone-based compounds in the relentless battle against cancer.[15]

Another interesting scaffold to explore in the design of hybrid compounds is the organochalcogens.[16,17] Sulfur, selenium, and tellurium-containing compounds have been important subjects of investigation due to their expressive number of pharmacological properties.[18,19] Among them, antimicrobial,[20] anticancer cell proliferation,[21,22] anti-HIV,[23] anti-Alzheimer's,[24] and potential infection control by SARS-CoV-2 can be highlighted.[25] In this context, we would like to highlight the research developed by Gritzenco et al.[26] where the authors obtained encouraging results regarding the alkynyl selenide compounds as a potential anticancer agent (Figure 1b) and the recent successful examples of selenium molecules against breast cancer (Figure 1c).[27,28] Regarding the above-mentioned, the combination of alkynyl-chalcogens with naphthoquinones may yield promising anticancer molecules.

https://doi.org/10.1021/acsomega.3c10134
ACS Omega 2024, 9, 21948−21963

Table 1. Optimization of Reaction Parameters[a]

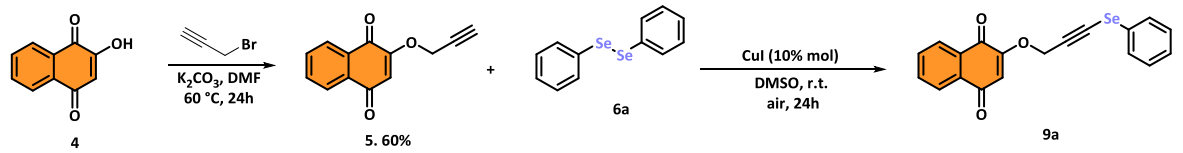

entry	$(PhSe)_2$ (equiv)	CuI (% mol)	base (equiv)	temp. (°C)	solvent	yield (%)
1	0.6	10	-	rt	DMSO	43
2	0.6	10	-	50	DMSO	38
3	0.6	10	-	80	DMSO	41
4	0.5	10	-	rt	DMSO	54
5	0.4	10	-	rt	DMSO	50
7	0.7	10	-	rt	DMSO	64
8	0.8	10	-	rt	DMSO	72
9	**0.9**	**10**	-	**rt**	**DMSO**	**85**
10	1.0	10	-	rt	DMSO	81
11	0.9	10	-	rt	DMSO	71[b]
12	0.9	10	$NaHCO_3$ (1.5)	rt	DMSO	64
13	0.9	10	K_2CO_3 (1.5)	rt	DMSO	85
14	0.9	10	Et_3N (1.5)	rt	DMSO	20
15	0.9	5	-	rt	DMSO	75
16	0.9	15	-	rt	DMSO	59
17	0.9	10	-	rt	DCM	-
18	0.9	10	-	rt	MeCN	traces
19	0.9	10	-	rt	EtOH	-
20	0.9	10	-	rt	DMF	traces
21	0.9	CuCl (10)	-	rt	DMSO	traces
22	0.9	CuO (10)	-	rt	DMSO	-

[a]Reaction conditions: propargyl alkylated lawsone **5** (0.25 mmol). [b]Inert atmosphere (nitrogen).

In this way, we proposed synthesizing a series of new hybrid substances containing naphthoquinone scaffolds derived from lawsone (**4**) and organochalcogens to evaluate their anticancer activity (Scheme 1). This endeavor is fueled by the pressing urgency posed by OSCC, which ranks as a significant global health concern. Therefore, this research is committed to pioneering the development of novel compounds with potential anticancer properties, focusing particularly on those exhibiting heightened activity and selectivity. We believe that these synthesized compounds have the potential to provide a much-needed breakthrough in addressing the seriousness of OSCC, furthering our pursuit of new cancer therapy solutions.

2. RESULTS AND DISCUSSION

2.1. Reaction Condition Optimization and Substrate Scope. The first step in the proposed synthetic route is to obtain propargyl alkylated lawsone (**5**) from a commercially available starting material (**4**). Following the procedure reported by Rocha et al.,[29] a 60% yield was achieved, using propargyl bromide, potassium carbonate, and dimethylformamide (DMF) as solvent for 24 h at 60 °C. Concurrently, diorganoyl dichalcogenides (**6a−i**) and (**7a−c**) could be synthesized using a well-established method described in existing literature.[30] This approach involves the reaction of bromobenzene (potentially substituted) to generate the Grignard reagent, which subsequently leads to the formation of the desired product, as previously outlined.

Subsequently, for the synthesis of the target molecules, a standard reaction was carried out with 0.25 mmol of (**5**) and 0.6 equiv of diphenyl diselenide (**6a**), 10 mol % of copper iodide (CuI), and 2.0 mL of DMSO, based on an experimental procedure previously reported.[25] Through these conditions plus room temperature and agitation on the bench, the product (**9a**) was obtained with a yield of 43% after 24 h of reaction (Table 1, entry 1).

In light of this outcome, various reaction parameters—including the quantity of diphenyl diselenide, catalyst, base, temperature, and solvents—were thoroughly examined (Table 1). When the interference of temperature in the performance of the reaction was evaluated at 50 and 80 °C, a decrease in the yield of the product was observed: 38% and 41%, respectively (Table 1, entries 2 and 3). Once the amount of diphenyl diselenide equivalents in the medium was assessed, we observed an inconsistency in the results. Both the increase and decrease of equivalents resulted in an improvement in the yield of the final product, with 85% being the best yield obtained in the presence of 0.9 equiv of dichalcogenide (Table 1, entries 4−10). The condition under an inert atmosphere was also evaluated; however, the yield produced was not considerably higher than that under normal conditions. This leads to the conclusion that the inert environment did not significantly increase the reaction yield (Table 1, entry 11). As a result, this quantity was chosen to remain constant during the subsequent optimization steps. In the next test, to achieve a better performance of the reaction, it was decided to use a base (Table 1, entries 12−14). By this protocol, only 1.5 equiv of K_2CO_3 was efficient, matching even the best yield found up to this point (85%).

The amount of CuI equivalents was also evaluated, and neither the increased nor the decreased amounts were beneficial to the reaction (Table 1, entries 15 and 16). The interference of the solvent in the progress of the reaction was

https://doi.org/10.1021/acsomega.3c10134
ACS Omega 2024, 9, 21948−21963

Scheme 2. Variation of Reaction Scope

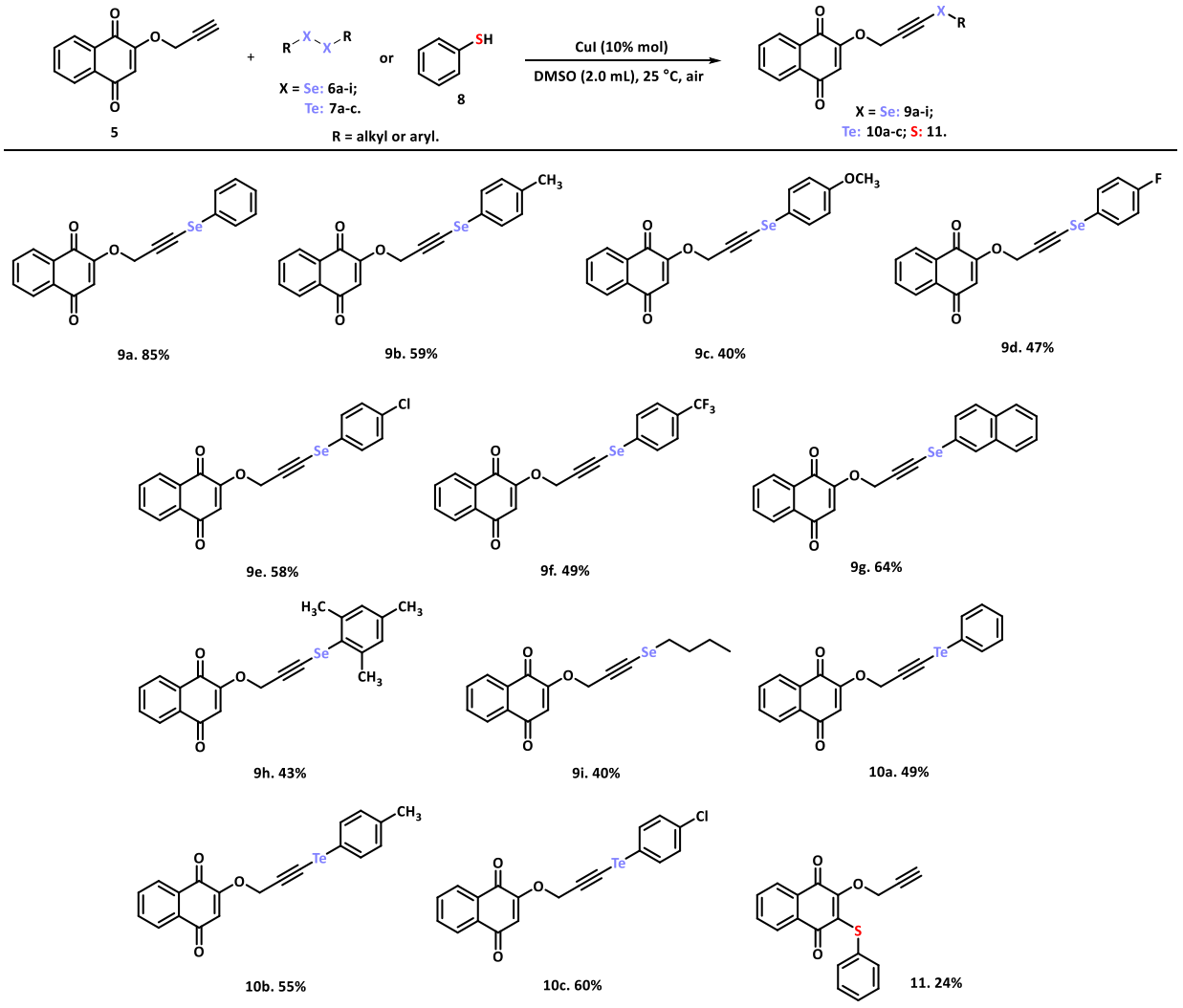

also investigated, and among those tested—dichloromethane (DCM), acetonitrile (MeCN), ethanol (EtOH), and dimethylformamide (DMF)—none of them proved to be as efficient as DMSO, since the product of interest was not obtained (Table 1, entries 17−20). Finally, screening for copper salts was performed, and both chloride and copper oxide were unfavorable for the reaction (Table 1, entries 21 and 22).

As a result of these screenings, the best reaction conditions were determined to be 0.25 mmol of propargylated lawsone (**5**), 0.9 equiv of diphenyl diselenide (**6a**), 10 mol % CuI, at room temperature for 24 h, yielding product (**9a**) with an 85% yield (Table 1, entry 9).

After establishing the optimized parameters to produce the new 2-((3-(phenylselanyl)prop-2-yn-1-yl)oxy)naphthalene-1,4-dione (**9a**), the scope of the proposed protocol was evaluated. In the initial phase of our research, we conducted reactions between various diorganoyl dichalcogenide structures (**6a−i** and **7a−c**), thiophenol (**8**), and propargylated lawsone (**5**). This synthesis approach resulted in the production of a diverse set of compounds, namely, organochalcogen-containing propargyl-naphthoquinones (**9a−i**, with X = Se), (**10a−c**, with X = Te), and (**11**, with X = S), as outlined in Scheme 2.

As shown in Scheme 2, the electron-donating substituents ($-CH_3$ and $-OCH_3$) in the aryl fraction of diselenides decreased the yield of the final molecules, resulting in moderate to good yields (59 and 40%) for the (**9b−c**) products. For the electron-withdrawing substituents (−F, −Cl, and $-CF_3$), only product (**9e**) yielded a moderate yield (−Cl, 58%), while products (**9d**) and (**9f**) yielded less satisfactory results compared to the test reaction (47% for −F and 49% for $-CF_3$). When diselenides featuring bulky substituents such as naphthyl (**6g**) and 1,2,3-triCH_3 (**6h**), interesting findings emerged. Notably, the reaction involving the former yielded a modest 43% yield (**9g**), while the latter resulted in a more favorable yield of 64% (**9h**). This observation suggests that steric effects do not significantly influence the reaction outcome. Furthermore, utilizing dibutyl diselenide (**6i**), 2-((3-(butylselanyl)prop-2-yn-1-yl)oxy)naphthalene-1,4-dione benzoate (**9i**) with an alkyl group immediately linked to the selenium atom, resulted in a 40% yield. It should be highlighted that the developed methodology was tolerant to a significant number of different diselenides.

To investigate the tolerance of the developed methodology as well as the biological effect of different chalcogens on the target structure, the reaction was performed with three diorganoyl ditellurides (**7a−c**) and with thiol (**8**). In this

https://doi.org/10.1021/acsomega.3c10134
ACS Omega 2024, 9, 21948−21963

Table 2. IC_{50} Results for SSC9 and NIH3T3 with Selectivity Index (S.I.) for New Compounds

SSC9 −oral squamous cell carcinoma			NIH3T3 −normal mouse fibroblasts			
compound	IC_{50} (μM)	R^2	compound	IC_{50} (μM)	R^2	S.I.
9a	31.91	0.85	**9a**	83.58	0.67	2.62
9b	17.09	0.98	**9b**	8.93	0.80	0.52
9c	24.76	0.98	**9c**	27.15	0.85	1.10
9d	23.49	0.92	**9d**	24.15	0.84	1.03
9e	65.36	0.97	-	-	-	-
9f	31.73	0.91	**9f**	56.53	0.81	1.78
9g	68.15	0.85	-	-	-	-
9h	48.95	0.89	-	-	-	-
9i	37.42	0.86	-	-	-	-
10a	1.648	0.97	**10a**	5.83	0.96	3.53
10b	4.001	0.94	**10b**	2.27	0.92	0.57
10c	2.885	0.94	**10c**	4.90	0.88	1.70
11	62.26	0.88	-	-	-	-
carboplatin	571.9	0.91	**carboplatin**	155.70	0.85	0.27
doxorubicin	2.705	0.96	**doxorubicin**	1.66	0.99	0.61

way, we expanded the compound library, including the synthesis with these chalcogen derivatives. In this case, **10a−c** and **11** were obtained in moderate to good yields. Diorganoyl ditellurides belonging to the category featuring an electron-withdrawing group (chlorine, **7c**) exhibit the highest yield of 60% (**10c**). Subsequently, the compound containing an electron-donating group, specifically a methyl group (**10b**), achieved a yield of 55%. Lastly, ditelluride devoid of substituents on the aromatic ring demonstrated a moderate yield of 49% (**10a**), suggesting a consistent profile, as the influence of substituents is not very evident.

To our surprise, the desired product was not obtained when diphenyl disulfide was used. Nonetheless, a change in the source of sulfur was performed to investigate this class of sulfur-containing compounds further. Thus, thiophenol (**8**) was used as a chalcogen source, and contrary to expectations, compound (**11**) was obtained in 24% yield. It is worth highlighting a key insight from prior research: the chemoselective addition of nucleophiles to the quinone core is higher when using thiols compared to the propargylated portion, indicating a remarkable preference for certain nucleophiles toward the quinone nucleus. This chemoselective behavior underscores the specificity and potential applications of nucleophilic additions to the quinone core, a finding of significance in our investigations. Given the intriguing nature of this structure from both synthetic and biological perspectives, ongoing research aims to validate additional potential applications.

Thus, we present an efficient catalytic method for promoting carbon-chalcogen bond synthesis by mildly reacting prop-2-yn-1-yl naphthoquinone derivatives with various substituted dichalcogenides. Under base-free circumstances, reactions were carried out at room temperature and in an open atmosphere. The integration of both organochalcogen moieties of diorganoyl dichalcogenides in the target product structures offers this synthetic process an atom-economic feature.

2.2. Biological Evaluation. *2.2.1. Cytotoxicity and Selectivity of the New Compounds.* To evaluate the potential antineoplastic properties of the newly synthesized chalcogen-naphthoquinone compounds in OSCC, we initially performed an MTT cell viability assay, which is based on the conversion of the tetrazolium compound MTT in insoluble formazan crystals by mitochondria of viable cells.[31] The biological activity of the 13 synthesized samples (**9a−i**, **10a−c**, and **11**) was assessed in SCC-9 cells derived from human tongue OSCC and previously described as more sensitive to cytotoxic agents than other SCC cell lines.[32,33] NIH3T3 mouse fibroblast cells were used as the normal cell control. The chemotherapy drug carboplatin, the gold standard in the treatment of oral cancer,[34,35] and doxorubicin, a naphthoquinone commonly used in some cancers,[36,37] were both used as positive controls for cytotoxicity. All 13 compounds displayed dose-dependent cytotoxicity in SCC9 cells, with higher biological activity than carboplatin, and their IC_{50} values are presented in Table 2. Interestingly, the three compounds derived from diorganoyl ditelluride reactions (**10a−c**) showed higher cytotoxicity in SCC-9 cells than derivatives from diorganoyl diselenides (**9a−i**) or thiophenol (**11**).

Of the 13 compounds tested in SSC-9 cells, eight (**9a−d**, **9f**, **10a−c**) were selected for their lower IC_{50} value in SCC-9 cells and subsequently tested along with carboplatin on the untransformed mouse fibroblast cell line NIH3T3 to evaluate their selectivity index (S.I.). This degree of selectivity can be used to screen the antineoplastic usefulness of certain compounds, in which a high S.I. value ≥ 2 represents a selective toxicity toward cancer cells, whereas a S.I. < 2 indicates a high chance of general toxicity of a compound, damaging both cancer and normal cells.[38] Table 2 shows that, as seen in SCC-9 cells, all eight chalcogen-naphthoquinones tested displayed biological activity higher than that of carboplatin. Once again, the three compounds derived from diorganoyl ditelluride reactions (**10a−c**) showed higher cytotoxicity in NIH3T3 than most of the five derivatives from diorganoyl diselenides. Finally, Table 2 summarizes the S.I. for all eight compounds tested plus carboplatin, in which we highlight the compounds (**9a**) (S.I.: 2.62) and (**10a**) (S.I.: 3.53) that were the most selective among all tested chalcogen-naphthoquinones. However, all new compounds were even more selective than carboplatin (S.I.: 0.27) and most to doxorubicin (S.I.: 0.61).

2.2.2. Wound Healing Assay. Activation of invasion and metastasis is one of the major characteristics involved in cancer development.[39,40] For carcinomas, such as OSCC, loss of epithelial traits is accompanied by increased cell migration as one of the several steps toward a metastasis event.[41] The wound healing or scratch assay is a simple, low-cost, and well-

https://doi.org/10.1021/acsomega.3c10134
ACS Omega 2024, 9, 21948−21963

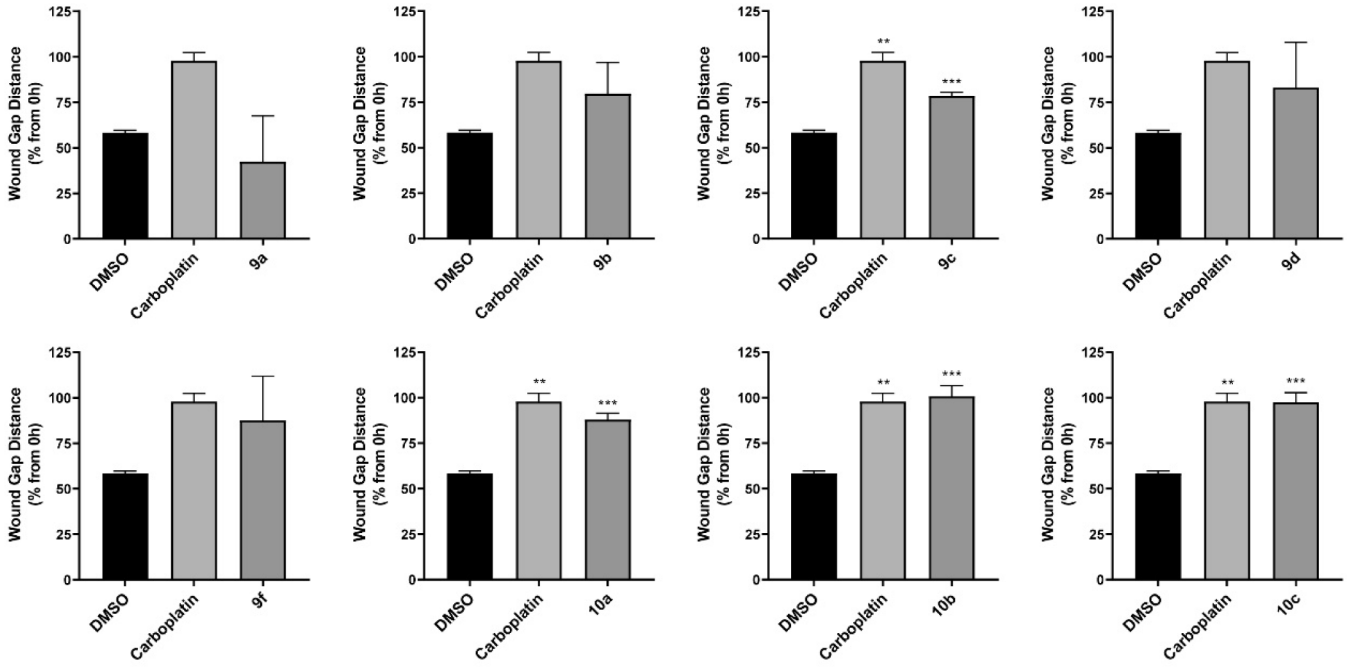

Figure 2. Effect of chalcogen-naphthoquinones on scratch area recovery of the oral squamous carcinoma cell culture. Asterisks (*) represent significant difference in values from the DMSO control (**, $p < 0.01$; **, $p < 0.001$).

developed method to measure cell migration *in vitro*.[42] The basic steps involve creating a scratch in a monolayer of cells, treating, and finally capturing the images at the beginning and regular intervals during the cell migration toward the scratch, and comparing the images to quantify the migration rate of the cells (images available in Figures S42 and S43). We observed that treatment with some of the newly synthesized chalcogen-naphthoquinones (**9c**, **10a−c**), as well as doxorubicin, significantly reduced the area recovered from the scratch after 24 h when compared to the negative control (Figure 2). Very little effect was observed after only 12 h of incubation (data not shown). We must highlight that this assay was conducted with a low serum concentration (5% v/v) to ensure that scratch recovery was due to cell migration and not cell proliferation, hence demonstrating a potential role of these chalcogen-naphthoquinones in hampering the risk of OSCC metastasis.

2.2.3. Cell Cycle and Cell Death Analysis. Both activation of cell death pathways and cell cycle arrest are defense mechanisms present in healthy cells to avoid propagation of genetic errors that could, over time, accumulate and support cancer development.[43,44] Yet, these same mechanisms can be targeted in cancer cells by chemotherapeutic compounds to treat cancer effectively. To evaluate the effects on both cell cycle and cell death caused by the newly synthesized chalcogen-naphthoquinones, we performed a flow cytometry analysis of SCC9 cells using propidium iodide, a well-known nucleic acid marker used for cell cycle progression or cell death studies. By staining cells with propidium iodide, we can quantify DNA to evaluate cell distribution in different cell cycle phases and cell death through DNA fragmentation.[45] SCC-9 cells were analyzed 48 h after treatment with DMSO (negative control), doxorubicin (positive control), or each of the eight selected compounds (**9a−d**, **9f**, **10a−c**) (Figure 3a). Interestingly, two compounds derived from diorganoyl ditellurides (**10a** and **10b**) significantly decreased the proportion of cells in the G_0/G_1 phase and increased DNA fragmentation compared to the negative control, with no apparent alteration in the percentage of cells in the G_2/M phases (Figure 3b). These results suggest that cells treated with these two compounds might not have finished cell cycle progression, possibly due to a certain degree of genotoxicity to SCC-9 cells. This can be a consequence of, for example, the formation of DNA adducts or the production of reactive oxygen species (ROS) by these compounds. Doxorubicin, known to cause DNA damage through topoisomerase-II disruption and generation of ROS,[46] also showed similar results (Figure 3b). Both effects have also been pointed out as mechanisms of action for naphthoquinones' antineoplastic activity.[15,47] In fact, an increase in ROS production is a valuable mechanism for antineoplastic drugs since cancer cells are presumably closer to a critical redox threshold at which apoptosis is induced.[48] Also, some effects of Se- and Te-based compounds on ROS production in cancer cells were discussed previously.[48,49] Finally, a tellurium-containing amphipathic compound induced $O_2^{\bullet-}$ production and oxidative stress in colon cancer cells, whereas its selenium counterpart was not able to do the same,[50] corroborating the data presented in our work.

The other six compounds tested (**9a−d**, **9f**, and **10c**) also increased DNA fragmentation, as seen in Figure 3c, with a marked reduction of cells in the G_2/M phases after 48 h of treatment. Moreover, cells treated with compounds (**9c**) and (**9f**) showed increased numbers of cells in the G_0/G_1 phase, suggesting a delay in cell cycle progression or activation of a cell cycle arrest mechanism (Figure 3c). Interestingly, inducing temporary cell cycle arrest is an emerging strategy in chemotherapy, as this approach is thought to prevent toxicity in normal cells such as hematopoietic and epithelial precursors.[51] Finally, all compounds tested showed increased DNA fragmentation in SCC-9 cells after 48 h of treatment, which confirms our previous data from the MTT viability

https://doi.org/10.1021/acsomega.3c10134
ACS Omega 2024, 9, 21948−21963

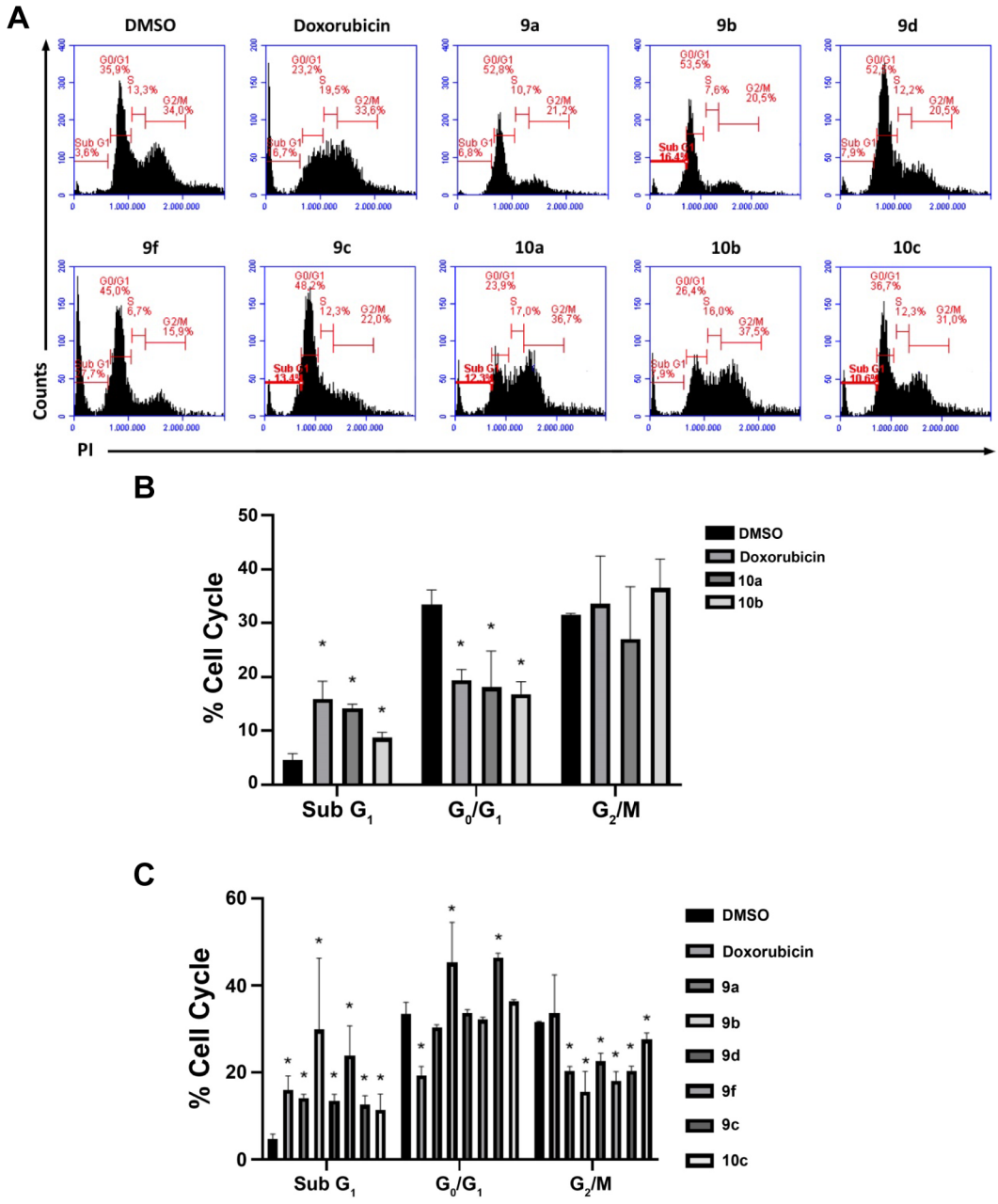

Figure 3. Effect of chalcogen-naphthoquinones on cell cycle progression and cell death in oral squamous carcinoma cells. Histogram charts (A) and column graphs (B and C) display the percentages of cell cycle distribution and Sub G1 DNA content of treated SCC9 cells. Asterisks (*) represent significant difference in values compared to control ($p < 0.05$).

assay. However, DNA fragmentation alone is not enough to clarify the exact cell death pathway activated by these chalcogen-naphthoquinones.

In recent decades, studies have demonstrated the anticancer potential of naphthoquinones, with some targets already described as DNA damage through the formation of ROS and suppressing topoisomerase-II, as well as controlling the tumor suppressor protein p53.[52] In this work, the combination of 1,4-naphthoquinone and a selenium or tellurium group in the same molecule was a strategy used to obtain hybrid compounds with potential and selective antineoplastic activity *in vitro* and lower toxicity than the compounds commonly used in cancer therapeutics. Several studies indicate that selenium-based compounds induce cell death by apoptosis and that mitochondria could be the target of these compounds.[53] Selenium also acts on other apoptotic mechanisms, such as the regulation of the appearance of glutathione and the generation of ROS.[48] Selenium plays an important role in the cell cycle and apoptosis, but these mechanisms are extremely complex and have not yet been fully elucidated.[54] As for tellurium, studies evaluating its biological activity are still scarce, although antineoplastic effects from tellurium compounds are believed to be associated with ROS formation, cell cycle arrest, induction of programmed cell death, and may have immunomodulatory effects,[55] being a class of compounds with great potential to be explored for the development of new anticancer molecules.[56] In this work, we could observe biological activity from all synthesized chalcogen-naphthoquinones derived from both diorganoyl diselenides and diorganoyl ditellurides, with an impact on cell migration, proliferation, and

https://doi.org/10.1021/acsomega.3c10134
ACS Omega 2024, 9, 21948−21963

overall survival in OSSC cells. Also, tellurium-derived compounds, especially the compound (**10a**), showed an increased antineoplastic potential with sufficient selectivity in relation to nontumor cells. Since OSSC still presents itself as a challenging malignancy for effective treatment,[57,58] several studies are being conducted to evaluate new synthetic or derivatives of natural compounds to improve OSSC prognosis and reduce chemotherapy comorbidities.[32,59] Considering the promising results obtained in terms of synthesis, yields, antiproliferative activity, cell migration inhibition, induction of cell death, and low toxicity, this work suggests the potential of the compound (**10a**) as a promising antineoplastic agent for further study.

2.3. Molecular Docking. In molecular docking studies, compound (**10a**) binds to and inhibits the polymerization of tubulin, thereby inhibiting the formation of microtubules acting on the mitotic spindles that form in mitosis. This prevents cell division and, consequently, induces apoptosis,[60] which is consistent with the results of the cell cycle analysis. Figure 3 shows that the cell reaches G2 but does not divide, probably due to the action of forming microtubules.

The development of new drugs is a complex process, where in addition to potency and selectivity the physicochemical characteristics of the molecule are important to predict the characteristics of the pharmacokinetics of the molecule. Thus, this molecule (**10a**) presents adequate characteristics to become a possible drug when analyzing the results of ADMET (absorption, distribution, metabolism, excretion, and toxicity), with the bonus of not being a substrate for P-glycoprotein. P-glycoprotein is linked with tumor resistance to multiple drugs since drugs that are substrates of P-glycoprotein may have their bioavailability decreased, impairing therapeutic efficacy.[61,62]

Initially, 6S8K redocking of all scoring functions (GoldScore, ChemScore, ASP, and ChemPLP) was performed with (3*Z*,6*Z*)-3-benzylidene-6-[(5-*tert*-butyl-1*H*-imidazol-4-yl)-methylidene]piperazine-2,5-dione (Plinabulin; PN6501). All functions showed RMSD (root mean square deviation) lower than 1 Å, and ChemPLP demonstrated the best RMSD (0.2339 Å) (Figure S44).

Several compounds in the series presented higher scores than the cocrystallized ligand, such as (**9a−b**, **9d−e**, **9g**) and (**10a−c**). In the ChemPLP scoring function, scores varied between 50.39 and 71.29, with the cocrystallized ligand presenting a score of 65.80, as shown in Table 3. The average presented for this series was 65.36.

The interactions that were observed between 6S8K and (**9e**) were mostly of the alkyl type, with a pi−sulfur-type interaction in the naphthoquinone-derived part of the structure (Cys241 residue). In (**9g**), the majority of interactions was also of the alkyl type; however, two hydrogen bonds were observed (Tyr202 and Leu242), both with the ligand acting as an H-receptor (Figure S45).

Compound (**9a**) showed a pi−sigma-type interaction with the naphthoquinone-derived part of the ligand (Leu255 residue), with the rest of the interactions being alkyl-type. For compound (**9b**), which had the highest score in the series, all interactions presented were of the alkyl type. However, nine favorable interactions were demonstrated. These interactions increase the stability of the compound at the active site (Phe169, Leu252, Val238, Leu242, and Leu255, Ala354, Cys241, Ala316, and Met259). Structure (**9d**) showed alkyl-type interactions with residues Leu252, Val238, Leu242, Leu255, Met259, Ala316, and Ala354. Leu255 also showed a pi−sigma interaction, according to compound (**9a**). The π−sulfur-type interaction with the Cys241 residue occurs according to several compounds of the series. Furthermore, a fluorine-type interaction was shown with the Gln136 residue (Figure 4).

In the semimetal derivatives, an unfavorable interaction (bump) with tellurium was observed in (**10a**) and (**10b**), with residue Val238. Despite this, the high score can be explained by the large number of alkyl-type interactions in both ligands. Together, $\pi-\sigma$ and $\pi-\pi$ stacked interactions were observed between Leu255 and Phe169, respectively, for (**10a**) and (**10b**). Cys241 still performed an π−sulfur-like interaction with (**10a**) (Figure 5). A high S.I. was observed concomitantly with an inhibition score higher than that of the cocrystallized ligand in molecular docking, placing **10a** as a probable tubulin inhibitor.

The exploration of tellurium derivatives as potential anticancer agents has captured considerable attention due to the distinctive chemical properties of this chalcogen. For example, studies conducted by Tripathi et al.[63] have already showcased the synthesis of telluroamino acids, demonstrating remarkable anticancer efficacy specifically against the MCF-7 breast cancer cell line. Additionally, research by Barcellos et al.[64] has emphasized the pro-oxidant activity of organo-tellurium compounds, suggesting their potential to induce apoptosis in malignant cells.

However, it is essential to acknowledge the challenges associated with employing molecular docking techniques to analyze tellurium compounds. The intricate and nuanced interactions between tellurium and biomolecules, coupled with the limited availability of robust analytical methods, present substantial obstacles in precisely determining dosages and administration routes in experimental models. While docking studies provide valuable insights into potential interactions, their predictive accuracy for tellurium compounds remains constrained due to the unique characteristics of tellurium's chemical behavior. Therefore, an integrative approach that combines computational docking with experimental validation is imperative to enhance the reliability and interpretation of results in the evaluation of the anticancer potential of tellurium derivatives.

2.4. *In Silico* Analysis of Physicochemical Properties. In addition to efficacy, potency, and safety, the pharmacokinetic and physicochemical properties of candidate molecules are also important variables in the drug discovery process. Through the analyses performed, the polar topological surface

Table 3. Scores Obtained for New Chalcogen-Functionalized Naphthoquinones via Molecular Docking Using GOLD Software with ChemPLP Function (PDB ID: 6S8K; Tubulin)

ID	ChemPLP	ID	ChemPLP
9a	67.39	**9g**	66.09
9b	71.29	**9h**	62.51
9c	65.37	**9i**	65.34
9d	69.03	**10a**	68.50
9e	67.68	**10b**	69.45
9f	59.91	**10c**	66.79
PN6501	65.80	**11**	50.39

https://doi.org/10.1021/acsomega.3c10134
ACS Omega 2024, 9, 21948−21963

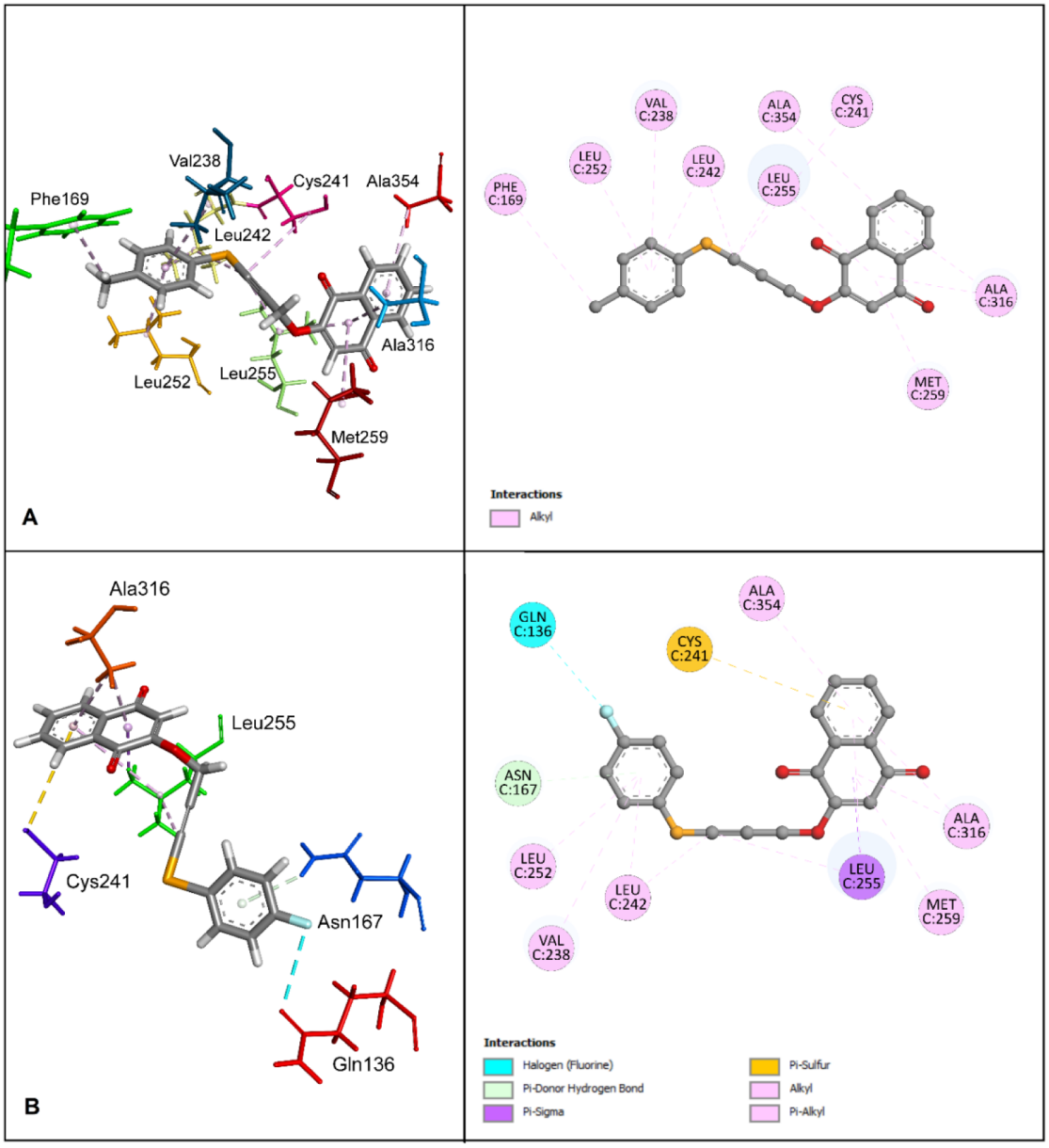

Figure 4. (A) 3D view and 2D diagram of ligand−receptor interactions between the tubulin protein and (**9b**). (B) 3D view and 2D diagram of ligand−receptor interactions between tubulin protein and (**9d**) (PDB ID: 6S8K; resolution: 1.52 Å).

area value of **10a** was 43.37 Å^2, while doxorubicin was 206.07 Å^2, as described in Table 4.

Compound **10a** presented moderate aqueous solubility, like the chemotherapy drug doxorubicin, which is highly absorbed in the intestine. It is not a substrate of P-glycoprotein, different from doxorubicin, but an inhibitor of the enzyme CYP1A2 (Table 5).

Lipinski's principle determines four physicochemical parameters as predictors of good oral absorption, in which a candidate cannot have more than one violation.[67] Compound **10a** showed no violations, while doxorubicin showed three violations (MLogP ≥ 4.15, number of electron acceptors >10, number of electron donors >5) (Table 6).

Given the data obtained in this study, it can be observed that both the naphthoquinone group and the tellurium group are important for anticancer activity. Naphthoquinones are used as feedstock for pharmaceuticals as well as for agrochemicals and other functional chemicals. The acid−base properties and the presence of two carbonyl groups that can accept one and/or two electrons to form the corresponding radical anion or dianion species are responsible for the biological activities of this class of compounds.[68] These compounds already present their representatives in the treatment of some types of cancer, such as doxorubicin, mitoxantrone, and daunorubicin.

When we think of molecules conjugated with tellurium, the conjugate with the best anticancer potential in this study, data in the literature are scarce. Selenium-containing compounds have exhibited a broad spectrum of activities that make them attractive in the search for new compounds with anticancer activity in medicinal chemistry, and as selenium, certain tellurium-containing compounds also exhibit the potential to form conjugates for the development of new drugs.[69] The search for these new conjugates for cancer treatment is important for the development of molecules that can circumvent the resistance of some to multiple drugs, as well as with less toxicity to nontumor cells, and that can also act on

https://doi.org/10.1021/acsomega.3c10134
ACS Omega 2024, 9, 21948−21963

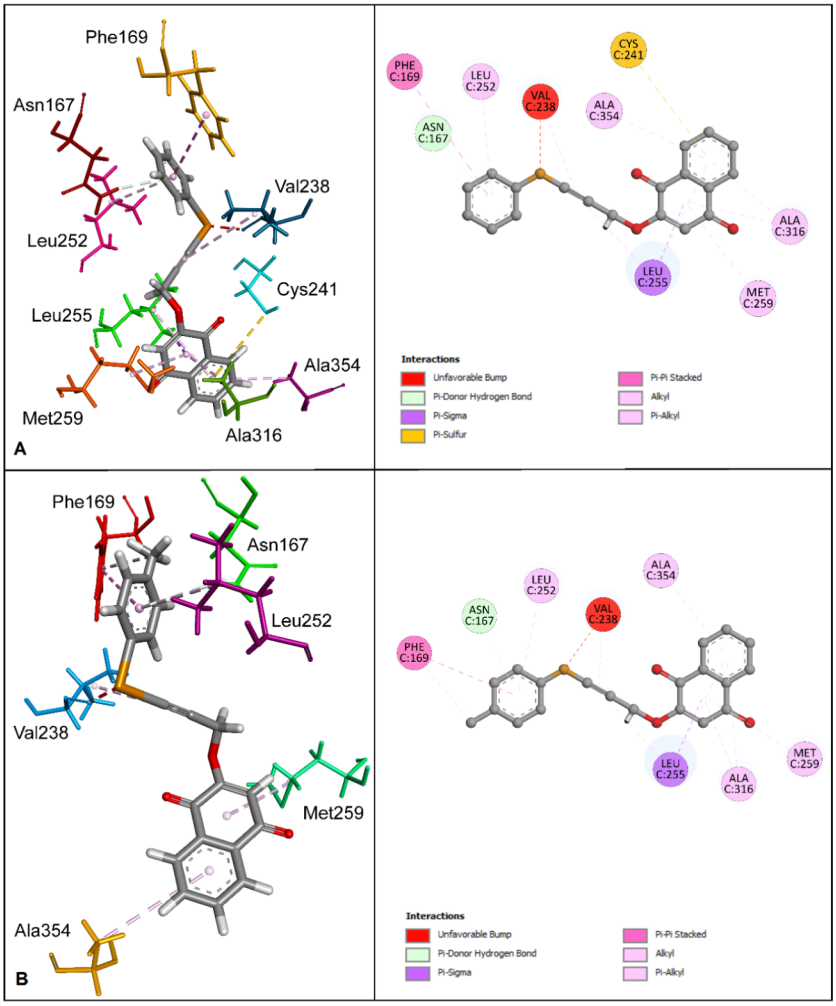

Figure 5. (A) 3D view and 2D diagram of ligand−receptor interactions between tubulin protein and **10a**. (B) 3D view and 2D diagram of ligand−receptor interactions between tubulin protein and **10b** (PDB ID: 6S8K; resolution: 1.52 Å).

Table 4. Physicochemical Properties and Lipophilicity

Molecule	MW[a]	TPSA[b]	# acceptors	# donors	$MLogP_{o/w}$[c]	$XLogP3_{o/w}$[d]
10a	415.90	43.37	3	0	2.05	3.52
doxorubicin	543.52	206.07	12	6	0.44	2.07

[a]Molecular weight g/mol. [b]Polar topological surface area in square Angstroms (Å^2). LogP = logarithm of the partition coefficient between octanol and water. [c]LogP calculated by the metholodogy of Lipinski et al.[65] [d]LogP calculated by Cheng's methodology.[66]

Table 5. Aqueous Solubility and Pharmacokinetic Parameters

molecule	Log *S*[a]	class	GI absorption[b]	P-gp[c]	CYP1A2[d]
10a	−4.82	moderately soluble	high	no	yes
doxorubicin	−5.2	moderately soluble	high	yes	no

[a]Aqueous solubility in mol/L calculated according to Ali's methodology. [b]Gastrointestinal absorption. [c]Substrate for P-glycoprotein (P-gp). [d]Human cytochrome P450 enzyme 1A2 (CYP1A2).

Table 6. Druglikeness and Leadlikeness

molecule	Lipinski[a]	Muegge[a]	bioavailability score[b]	leadlikeness[a]
10a	0	1	0.85	2
doxorubicin	3	3	0.17	1

[a]Number of violations. [b]Abbott bioavailability score that determines the probability of a molecule having more than 10% bioavailability in rats.

the primary tumor, reducing the risk of cell migration and the emergence of secondary tumors due to metastasis.

Compounds with selenium and tellurium have already demonstrated the potential to interact with P-glycoprotein,[70] just as our *in silico* studies predict. Studies with natural products and their derivatives that formed conjugates with selenium and tellurium against resistant cancers show that many derivatives containing these elements of chalcogen in their structure can reverse MDR (multidrug resistance) cancer via the inhibition of efflux pumps that are overexpressed in resistant cancers. In these types of cancers, the cells recognize the chemotherapy drugs and expel them out of the cells, preventing them from exerting their antitumor action.[67] Thus, these conjugates can reverse this resistance to multiple drugs

https://doi.org/10.1021/acsomega.3c10134
ACS Omega 2024, 9, 21948−21963

that are responsible for the failure to treat many patients with cancer, which can lead to death.

Thus, the development of MDR constitutes a primary impediment to the success of chemotherapy, where tumor stem cells are responsible for cancer progression and recurrence. Among various mechanisms of drug resistance, efflux pumps belonging to ATP binding transporters (ABCs) have been shown to be the most important contributors to MDR,[71,72] and the most extensively characterized MDR transporters include P-glycoprotein and multidrug-resistant protein 1 (also known as ABCC1 or MRP1).[73,74] The compound **10a**, the standout compound in our study, is not a substrate for P-glycoprotein and can circumvent tumor resistance to treatment.

Therefore, with *in silico* methodologies, such as molecular docking and ADME, we demonstrated that it is possible to use the molecules for subsequent *in vivo* studies, where there will be the possibility of the compound interacting with a living system with excellent potential for clinical studies.

3. CONCLUSIONS

In this work, we described the synthesis of 13 new chalcogen-propynyl-naphthoquinones (**9a−i**, **10a−c**, and **11**) with good to excellent yields using an efficient methodology at room temperature, under base-free and open-to-air atmosphere conditions. Notably, this newly developed series of hybrid compounds exhibits remarkable attributes, including air stability, ease of handling, and comprehensive characterization through ^{1}H and ^{13}C NMR spectroscopy as well as HRMS (high-resolution mass spectrometry) analyses. Furthermore, the antiproliferative experiments have revealed that these compounds have the potential to be effective anticancer cell growth agents. In particular, compounds **9a** and **10a** have shown greater selectivity, implying that they may have a higher anticancer efficacy while being less hazardous. This is consistent with Lipinski's rule, which states that compounds that meet certain physicochemical requirements have lower dropout rates during clinical trials and a higher probability of successful market penetration. In conclusion, this study highlights not only the synthesis of these interesting hybrid compounds but also their potential as important candidates in the pursuit of more effective and safer anticancer drugs, providing a ray of hope in the hunt for improved cancer therapies.

4. EXPERIMENTAL PROCEDURES

4.1. Chemistry. For the isolation and purification of the compounds using column chromatography, a glass column was used, silica gel was used as the stationary phase with a 0.063−0.2 mesh by Merck (Darmstadt, Germany), and a suitable solvent or solvent mixture was used as the eluent. The fractions and compounds obtained were analyzed by thin layer chromatography (TLC), using aluminum plates coated with silica gel 60 GF254 provided by Merck (Darmstadt, Germany), 0.25 mm thick, and with particles between 5 and 40 μm in diameter. The substances separated on the chromatographic plates were visualized using several development methods: in an iodine chamber, in an ultraviolet light chamber, or with a vanillin reagent followed by heating at 110 °C. Melting points were obtained on a Fisatom 430D apparatus and were uncorrected. All solvents and reagents used in the synthesis, purification, and characterization were purchased from commercial sources, Sigma-Aldrich, Merck (Darmstadt, Germany), and Synth (Sao Paulo, Brazil) and used without prior purification. APPI-Q-TOFMS measurements were taken on a mass spectrometer equipped with an automatic syringe pump for sample injection. The $^{13}C\{^{1}H\}$ NMR spectra were obtained on a Bruker Advance NEO spectrometer, operating at 500 MHz, employing a direct broadband probe at 125 MHz.

4.2. Synthetic Procedures. *4.2.1. General Procedure for the Synthesis of PropargylatedLawsone (**5**)* .[28] In a round-bottom flask, 5.75 mmol of lawsone (**4**), 1.2 equiv K_2CO_3, and 50 mL of DMF were mixed and allowed to stir for 15 min. Then, 10 equiv of propargyl bromide was added and heated at 60 °C for 12 h. Subsequently, after the mixture was cooled to room temperature, ethyl acetate was added to the mixture, and this phase was washed with brine (3 × 100 mL). The organic phase was dried with anhydrous sodium sulfate and filtered, and the solvent was evaporated under reduced pressure. The product was purified by column chromatography on silica gel using a gradient hexane/ethyl acetate mixture as an eluent.

4.2.1.1. 2-(Prop-2-yn-1-yloxy)naphthalene-1,4-dione. (Compound **5**). 0.732 g, yield 60%, yellow solid, mp 148 °C (lit. 150 °C)[28] ^{1}H NMR ($CDCl_3$, 500 MHz) δ (ppm) = 8.15−8.08 (m, 2H), 7.77−7.71 (m, 2H), 6.36 (s, 1H), 4.80 (d, J = 2.5 Hz; 2H), 2.65 (t, J = 2.5 Hz; 1H). $^{13}C\{^{1}H\}$ NMR ($CDCl_3$, 125 MHz) δ: 184.68, 179.79, 158.05, 134.36, 133.45, 131.88, 131.05, 126.73, 126.22, 111.65, 78.18, 75.43, 56.73.

*4.2.2. General Procedure for the Synthesis of 2-((3-(Organochalcogenyl)prop-2-yn-1-yl)oxy)naphthalene-1,4-dione (**9a−i,10a−c, and 11**)* .[25] At 25 °C, DMSO (1.0 mL) was added to a round-bottom flask containing the appropriate diorganoyl dichalcogenide (**6a−i**), (**7a−c**), and (**8**) (0.90 equiv) and CuI (10 mol %) under ambient atmosphere. Then, the propargylated lawsone (**5**) (0.25 mmol) diluted in DMSO (1.0 mL) was added to the stirred reaction mixture and stirred for 24 h. Thereafter, the mixture was extracted with sat. aq NH_4Cl (5.0 mL), EtOAc (3 × 5.0 mL), and dried over $MgSO_4$. Finally, after filtration, the organic solution was concentrated on a rotary evaporator at low pressure and purified by flash chromatography on silica gel with hexane/EtOAc as the eluent.

4.2.2.1. 2-((3-(Phenylselanyl)prop-2-yn-1-yl)oxy)-naphthalene-1,4-dione. (Compound **9a**). 0.0782 g, yield: 85%, yellow solid, mp 135 °C, ^{1}H NMR ($CDCl_3$, 500 MHz) δ = 8.07−8.01 (dd, J = 9.1 and 1.7 Hz; 2H), 7.70−7.63 (m, 2H), 7.44−7.41 (m, 2H), 7.27−7.18 (m, 3H), 6.30 (s, 1H), 4.93 (s, 2H). $^{13}C\{^{1}H\}$ NMR ($CDCl_3$, 125 MHz) δ = 184.65, 179.95, 158.13, 134.35, 133.43, 131.95, 131.08,129.74, 129.69, 127.68, 126.75, 126.22, 111.67, 95.36, 72.57, 57.85. HRMS (APPI+) m/z: calcd for $C_{19}H_{12}O_3Se$ $[M]^+$: 368.0106; found: 369.0181.

4.2.2.2. 2-((3-(p-Tolylselanyl)prop-2-yn-1-yl)oxy)-naphthalene-1,4-dione. (Compound **9b**). 0.0561 g, yield: 59%, orange solid, mp 115 °C, ^{1}H NMR ($CDCl_3$, 500 MHz) δ = 8.15−8.09 (dd, J = 9.1 and 1.8 Hz; 2H), 7.77−7.70 (td, J = 9.1 and 1.8 Hz; 2H), 7.41−7.36 (d, J = 8.3 Hz; 2H), 7.15−7.10 (d, J = 8.3 Hz; 2H), 6.36 (s, 1H), 4.98 (s, 2H), 2.33 (s, 3H). $^{13}C\{^{1}H\}$ NMR ($CDCl_3$, 125 MHz) δ = 184.06, 179.97, 158.14, 137.94, 137.01, 134.37, 133.44, 131.94, 131.12, 130.52, 130.42, 130.19, 130.11, 127.81, 127.42, 126.76, 126.23, 111.66, 94.69, 72.24, 57.91, 21.08. HRMS (APPI+) m/z: calcd for $C_{20}H_{14}O_3Se$ $[M + Na]^+$: 404.2765; found: 404.9988.

4.2.2.3. 2-((3-((4-Methoxyphenyl)selanyl)prop-2-yn-1-yl)-oxy)naphthalene-1,4-dione. (Compound **9c**). 0.0397 g, Yyeld: 40%, orange oil, ^{1}H NMR ($CDCl_3$, 500 MHz) δ =

https://doi.org/10.1021/acsomega.3c10134
ACS Omega 2024, 9, 21948−21963

8.12−8.07 (dd, J = 7.4 and 1.5 Hz; 2H), 7.76−7.69 (td, J = 7.4 and 1.5 Hz; 2H), 7.44 (d, J = 8.9 Hz; 2H), 6.85 (d, J = 8.9 Hz; 2H), 6.32 (s, 1H), 4.94 (s, 2H), 3.79 (s, 3H). $^{13}C\{^1H\}$ NMR ($CDCl_3$, 125 MHz) δ: 184.64, 179.95, 158.83, 158.13, 134.33, 133.40, 132.69, 131.92, 131.09, 126.72, 126.18, 116.91, 115.48, 111.62, 93.85, 73.71, 57.89, 55.38. HRMS (APPI+) m/z: calcd for $C_{20}H_{14}O_4Se$ $[M + Na]^+$: 413.2065; found: 413.2648.

4.2.2.4. 2-((3-((4-Fluorophenyl)selanyl)prop-2-yn-1-yl)-oxy)naphthalene-1,4-dione. (Compound **9d**). 0.0452 g, yield: 47%, yellow solid, mp 98 °C, ^1H NMR ($CDCl_3$, 500 MHz) δ = 8.15−8.09 (dd, J = 7.4 and 2.0 Hz; 2H), 7.77−7.72 (m, 2H), 7.51−7.48 (m, 2H), 7.06−7.03 (t, J = 8.6 Hz; 2H), 6.34 (s, 1H), 4.98 (s, 2H). $^{13}C\{^1H\}$ NMR ($CDCl_3$, 125 MHz) δ = 184.67, 179.95, 163.67 (d, J = 247.5 Hz; C_{arom}), 158.10, 134.42, 133.49, 132.31, 132.25, 131.92, 131.11, 130.17, 126.78, 126.25, 124.56 (d, J_{C-F} = 3.8 Hz; C_{arom}), 116.93 (d, J_{C-F} = 22.5 Hz; CH_{arom}), 111.65, 95.04, 72.71, 57.72. HRMS (APPI +) m/z: calcd for $C_{19}H_{11}FO_3Se$ $[M + Na]^+$: 408.2404; found: 408.9746.

4.2.2.5. 2-((3-((4-Chlorophenyl)selanyl)prop-2-yn-1-yl)-oxy)naphthalene-1,4-dione. (Compound **9e**). 0.0582 g, yield: 58%, orange solid, mp 145 °C, ^1H NMR ($CDCl_3$, 500 MHz) δ = 8.15−8.09 (dd, J = 7.5 and 1.4 Hz; 2H), 7.78−7.69 (m, 2H), 7.62−7.59 (d, J = 8.6 Hz; 2H), 7.26−7.24 (t, J = 8.6 Hz; 2H), 6.35 (s, 1H), 5.05 (s, 2H). $^{13}C\{^1H\}$ NMR ($CDCl_3$, 125 MHz) δ: 184.65, 179.92, 158.08, 134.42, 134.00, 133.50, 131.90, 131.04, 129.88, 126.77, 126.26, 125.58, 111.64, 95.81, 72.00, 57.77. HRMS (APPI+) m/z: calcd for $C_{19}H_{11}ClO_3Se$ $[M+K]^+$: 446.0112; found: 446.0439.

4.2.2.6. 2-((3-((4-(Trifluoromethyl)phenyl)selanyl)prop-2-yn-1-yl)oxy)naphthalene-1,4-dione. (Compound **9f**). 0.0533 g, yield: 49%, light yellow solid, mp 100 °C, ^1H NMR ($CDCl_3$, 500 MHz) δ = 8.13−8.07 (dd, J = 9.1 and 1.6 Hz; 2H), 7.74−7.70 (td, J = 9.1 and 1.6 Hz; 2H), 7.48−7.46 (m; 2H), 7.06−7.02 (t, J = 8.6 Hz; 2H), 6.32 (s, 1H), 4.96 (s, 2H). $^{13}C\{^1H\}$ NMR ($CDCl_3$, 125 MHz) δ = 184.63, 179.88, 158.09 (d, J_{C-F} = 5 Hz), 134.46 (d, J_{C-F} = 5 Hz), 133.53 (d, J_{C-F} = 3.8 Hz), 131.89, 131.08, 130.17, 129.15 (q, J_{C-F} = 36.3 Hz; C_{arom}), 126.79, 126.46 (q, J_{C-F} = 2.5 Hz; CH_{arom}), 126.44 (q, J_{C-F} = 295 Hz; CF_3), 126.28, 111.66, 96.92, 70.97, 57.71. HRMS (APPI+) m/z: calcd for $C_{20}H_{11}F_3O_3Se$ $[M + Na]^+$: 458.2482; found: 458.9655.

4.2.2.7. 2-((3-(Naphthalen-2-ylselanyl)prop-2-yn-1-yl)-oxy)naphthalene-1,4-Dione. (Compound **9g**). 0.0448 g, yield: 43%, greenish solid, mp 165 °C, ^1H NMR ($CDCl_3$, 500 MHz) δ = 8.12−8.05 (dd, J = 7.7 and 1.5 Hz; 2H), 8.00−7.98 (dd, J = 7.2 and 1.1 Hz; 1H), 7.92−7.90 (dd, J = 7.2 and 1.1 Hz; 1H), 7.82−7.80 (dd, J = 7.2 and 1.1 Hz; 1H), 7.75−7.68 (td, J = 7.7 and 1.5 Hz; 2H), 7.53−7.41 (m, 3H), 6.29 (s, 1H), 4.94 (s, 2H). $^{13}C\{^1H\}$ NMR ($CDCl_3$, 125 MHz) δ = 184.55, 179.96, 158.06, 134.34, 134.12, 133.41, 132.28, 131.93, 131.10, 130.38, 129.15, 128.78, 127.05, 126.73, 126.52, 126.20, 125.88, 125.76, 111.65, 94.79, 72.43, 57.86. HRMS (APPI+) m/z: calcd for $C_{23}H_{14}O_3Se$ $[M + Na]^+$: 440.3095; found: 440.9998.

4.2.2.8. 2-((3-(Mesitylselanyl)prop-2-yn-1-yl)oxy)-naphthalene-1,4-dione. (Compound **9h**). 0.0653 g, yield: 64%, light yellow solid, mp 165 °C, ^1H NMR ($CDCl_3$, 500 MHz) δ = 8.13−8.08 (dd, J = 7.3 and 1.8 Hz; 2H), 7.77−7.70 (td, J = 7.3 and 1.8 Hz; 2H), 6.93 (s, 2H), 6.26 (s, 1H), 6.36 (s, 1H), 4.84 (s, 2H), 2.52 (s, 6H), 2.27 (s, 3H). $^{13}C\{^1H\}$ NMR ($CDCl_3$, 125 MHz) δ = 184.65, 180.00, 158.19, 142.21, 139.65, 134.31, 133.37, 131.95, 131.11, 129.13, 126.72, 126.18, 124.75, 111.58, 89.71, 73.98, 58.01, 24.12, 20.95. HRMS (APPI+) m/z: calcd for $C_{22}H_{18}O_3Se$ $[M + Na]^+$: 432.3299; found: 433.0301.

4.2.2.9. 2-((3-(Butylselanyl)prop-2-yn-1-yl)oxy)-naphthalene-1,4-dione. (Compound **9i**). 0.0347 g, yield: 40%, reddish solid, mp 116 °C, ^1H NMR ($CDCl_3$, 500 MHz) δ = 8.15−8.08 (dd, J = 7.7 and 1.6 Hz; 2H), 7.77−7.70 (td, J = 7.7 and 1.6 Hz; 2H), 6.34 (s, 1H), 4.92 (s, 2H), 2.81 (t, J = 7.4; 2H), 1.79−1.73 (qt, J = 7.4 Hz; 2H), 1.46−1.38 (sxt, J = 7.4 Hz; 2H), 0,91 (t, J = 7.4 Hz; 3H). $^{13}C\{^1H\}$ NMR ($CDCl_3$, 125 MHz) δ: 184.70, 180.02, 158.19, 134.31, 133.37, 131.94, 131.12, 126.71, 126.18, 111.61, 92.02, 73.44, 58.00, 32.23, 29.24, 22.42, 13.42. HRMS (APPI+) m/z: calcd for $C_{17}H_{16}O_3Se$ $[M + Na]^+$: 370.2592; found: 371.0141.

4.2.2.10. 2-((3-(Phenyltellanyl)prop-2-yn-1-yl)oxy)-naphthalene-1,4-dione. (Compound **10a**). 0.0509 g, yield: 49%, yellow solid, mp 125 °C, ^1H NMR ($CDCl_3$, 500 MHz) δ = 8.14−8.08 (dd, J = 9.1 and 1.8 Hz; 2H), 7.77−7.70 (td, J = 9.1 and 1.8 Hz; 2H), 7.69−7.66 (m, 2H), 7,32−7,25 (m, 2H), 6.37 (s, 1H), 5.05 (s, 2H). $^{13}C\{^1H\}$ NMR ($CDCl_3$, 75 MHz) δ = 184.68, 179.98, 158.13, 135.83, 134.36, 133.43, 131.95, 131.12, 129.97, 128.43, 126.54, 126.21, 111.93, 111.69, 106.45, 58.01, 51.08. HRMS (APPI+) m/z: calcd for $C_{19}H_{12}O_3Te$ $[M + Na]^+$: 440.9698; found: 440.9753.

4.2.2.11. 2-((3-(p-Tolyltellanyl)prop-2-yn-1-yl)oxy)-naphthalene-1,4-dione. (Compound **10b**). 0.0591 g, yield: 55%, yellow solid, mp 142 °C, ^1H NMR ($CDCl_3$, 500 MHz) δ = 8.14−8.09 (dd, J = 7.7 and 1.5 Hz; 2H), 7.77−7.70 (td, J = 7.7 and 1.5 Hz; 2H), 7.60−7.58 (d, J = 8,1 Hz; 2H), 7.10−7.08 (d, J = 8.1 Hz; 2H), 6.35 (s, 1H), 5.03 (s, 2H), 2.35 (s, 3H). $^{13}C\{^1H\}$ NMR ($CDCl_3$, 125 MHz) δ = 184.69, 179.99, 158.14, 138.75, 136.49, 134.33, 133.41, 131.96, 131.13, 130.83, 130.17, 129.89, 126.74, 126.19, 111.69, 107.50, 105.82, 76.79, 58.03, 51.21, 21.20. HRMS (APPI+) m/z: calcd for $C_{20}H_{14}O_3Te$ $[M + Na]^+$: 454.9893; found: 454.9895.

4.2.2.12. 2-((3-((4-Chlorophenyl)tellanyl)prop-2-yn-1-yl)-oxy)naphthalene-1,4-dione. (Compound **10c**). 0.0675 g, yield: 60%, black solid, mp 160 °C, ^1H NMR ($CDCl_3$, 500 MHz) δ = 8.15−8.09 (dd, J = 7.5 and 1.4 Hz; 2H), 7.78−7.71 (td, J = 7.5 and 1.4 Hz; 2H), 7.62−7.59 (d, J = 8.6 Hz; 2H), 7.26−7.22 (d, J = 8.6 Hz; 2H), 6.35 (s, 1H), 5.05 (s, 2H). $^{13}C\{^1H\}$ NMR ($CDCl_3$, 125 MHz) δ = 184.64, 179.91, 158.07, 137.20, 135.04, 134.38, 133.45, 131.90, 131.08, 130.15, 129.87, 126.74, 126.23, 111.67, 109.40, 106.84, 57.91, 50.65. HRMS (APPI+) m/z: calcd for $C_{19}H_{11}ClO_3Te$ $[M + Na]^+$: 474.9330; found: 474.9335.

4.2.2.13. 2-(Phenylthio)-3-(prop-2-yn-1-yloxy)-naphthalene-1,4-dione. (Compound **11**). 0.0192 g, yield: 24%, orange oil, ^1H NMR ($CDCl_3$, 500 MHz) δ = 8.09−8.04 (m, 2H), 7.73−7.70 (m, 2H), 7.50−7.44 (dd, 2H), 7.31−7.27 (m, 3H), 4.98 (d, J = 2.5 Hz; 2H), 2.50 (t, J = 2.5 Hz; 1H). $^{13}C\{^1H\}$ NMR ($CDCl_3$, 125 MHz) δ = 184.65, 179.95, 158.11, 136.25, 134.40, 133.47, 131.92, 131.67, 131.26, 131.04, 129.92, 129.48, 127.22, 126.87, 126.77, 126.24, 111.62, 90.77, 78.90, 57.80. HRMS (APPI+) m/z: calcd for $C_{19}H_{12}O_3S$ $[M + Na]^+$: 343.0351; found: 343.0393.

4.3. Biological Evaluation. *4.3.1. Cell Lines and Reagents.* SCC-9 cells, derived from human tongue OSCC, were obtained from ATCC (CRL-1629) and maintained in 1:1 DMEM/F12 medium (Dulbecco's modified Eagle's medium and Ham's F12 medium); Gibco (Thermo Fisher, Waltham, MA, USA) supplemented with 10% (v/v) FBS (fetal bovine serum; Invitrogen, Thermo Fisher, Waltham, MA, USA) and

https://doi.org/10.1021/acsomega.3c10134
ACS Omega 2024, 9, 21948−21963

400 ng/mL hydrocortisone (Sigma-Aldrich Co., St. Louis, MO, USA). NIH3T3 mouse fibroblasts were obtained from ATCC (CRL-1658) and maintained in DMEM supplemented with 10% (v/v) FBS. The cells were cultured in a humidified environment containing 5% CO_2 at 37 °C. Carboplatin (Libbs Farmacêutica, São Paulo, SP, Brazil) and doxorubicin (Libbs Farmacêutica, São Paulo, SP, Brazil) were used as positive controls for gold standard antineoplastic drugs.

4.3.2. Cell Viability and Selectivity Index Calculation. SCC-9 cells or NIH3T3 fibroblasts (5×10^3 cells/well) were plated in triplicate in a 96-well plate and incubated as indicated with different concentrations of the compounds for 48 h. DMSO was diluted in culture medium at the same concentrations and used as a negative control, representing 100% cell viability. After 48 h of treatment, cells were incubated for 4 h with 5 mg/mL of MTT reagent (3,4,5-dimethiazol-2,5-diphenyltetrazolium bromide) (Sigma-Aldrich Co., St. Louis, MO, USA) diluted in culture medium. Subsequently, the formazan crystals were dissolved by MTT solvent (50% methanol and 50% DMSO), and the absorbance was read at 560 nm using an EPOCH microplate spectrophotometer (BioTek Instruments, Winooski, VT, USA) with the background absorbance at 670 nm subtracted. The S.I. was calculated as IC_{50} of the pure compound in a normal cell line NIH3T3/IC_{50} of the same pure compound in cancer cell line SCC-9.

4.3.3. Wound Healing Assay. SCC-9 cells were seeded in 24-well plates (7.5×10^4 cells/well) and cultured up to 80% confluence at 37 °C and 5% CO_2. A sterile tip was used to scratch the medial surface of each well, and cells were then maintained with reduced serum concentration (5% v/v) to avoid cell proliferation and treated with DMSO (negative control), carboplatin (positive control), or each of the chalcogen-naphthoquinones indicated. Doses for all substances were set at IC_{50} values for SCC-9 cells obtained in the cell viability assays. Images of the scratch were taken at the beginning (0 h) or 12 and 24 h after treatment using the Evos microscope XL Core Imaging System (Thermo Fisher Scientific, Oregon, USA), and the medium gap distance between wound margins for each image was measured using ImageJ software (National Institute of Health, Bethesda, MD, USA). Statistical analysis was performed using one-way ANOVA with Dunnett's multiple comparison test against DMSO control.

4.3.4. Cell Cycle Progression and Cell Death. SCC-9 cells were plated in 6-well plates (2×10^5 cells/well) cultured for 24 h and then treated with DMSO (negative control), carboplatin (positive control), or each of the chalcogen-naphthoquinones indicated for 48 h. Doses for all substances were set at IC_{50} values for SCC-9 cells obtained in cell viability assays. Cells were then trypsinized and stained with propidium iodide (0.02 mg/mL in Triton X-100 solution at 0.1%). The samples were incubated for 15 min at 37 °C, and DNA content was analyzed by collecting 10,000 events by flow cytometry in a BD Accuri C6 Plus system (BD Bioscience, San Jose, CA, USA). The data were analyzed using Cell Quest Pro software (BD Bioscience, San Jose, CA, USA). Statistical analysis was performed using one-way ANOVA with Turkey's multiple comparison test, where all columns were significantly different from the negative control.

4.3.5. Molecular Docking. To perform the molecular docking, the Hermes GOLD software (Genetic Optimization for Ligand Docking, version 2022.3.0) was used, based on the methodology of Verdonk et al.,[75] which uses a genetic-type algorithm for interaction between ligand and receptor. The chosen structure of the target, together with the cocrystallized ligand used, was 6S8K (structure, thermodynamics, and kinetics of plinabulin binding to two tubulin isotypes) deposited in the PDB (Protein Data Bank). The protein was prepared using the GOLD Wizard tool, excluding water molecules not belonging to the active site, the cocrystallized linker, and double conformations. Hydrogen atoms were added, and the active site was configured by selecting a 6 Å sphere from the points *X*: 16.3395, *Y*: −5.9471, and *Z*: 26.7009.

Protein preparation was performed using the APBS Biomolecular software at pH 7.4.[76,77] Rest of the settings were kept at default for the design of the Schiff bases, the ChemSketch 2021.1.1 software[78] was used, in which the SMILES codes were generated to generate the three-dimensional structure in Avogadro 1.2.0.[79] In Avogadro 1.2.0, a preoptimization was performed using the UFF force field until $\Delta E < 10^{-3}$ kJ mol^{-1}.

The configuration of the ligands was performed in MarvinSketch 22.11,[80] using the microspecies/pK_a distribution tool and setting the physiological pH (7.4),[74] with the rest of the configurations in default. Anchoring was performed using the GoldScore, ChemScore, ASP, and ChemPLP scoring functions. The solutions were visually inspected to analyze binding patterns, intermolecular interactions, and ligand positioning in the site.

4.3.6. In Silico Analysis of Physicochemical Properties. **10a**, the molecule with the greatest anticancer potential, had its physicochemical profile analyzed by the SwissADME program (http://www.swissadme.ch).[81]

■ ASSOCIATED CONTENT

Supporting Information

The Supporting Information is available free of charge at https://pubs.acs.org/doi/10.1021/acsomega.3c10134

Spectral data (^{1}H and ^{13}C{^{1}H} NMR, HRMS spectra) of **5**, **9a−i**, **10a−c**, **11** (Figure S1−S41); biological assay data (Figures S42 and S43); and molecular docking (Figures S44 and S45) (PDF)

■ AUTHOR INFORMATION

Corresponding Author

Vanessa Nascimento − *SupraSelen Laboratory, Department of Organic Chemistry, Institute of Chemistry, Federal University Fluminense, Niterói-RJ 24020-141, Brazil;* orcid.org/0000-0001-9413-7638; Email: nascimentovanessa@id.uff.br

Authors

Luana da Silva Gomes − *SupraSelen Laboratory, Department of Organic Chemistry, Institute of Chemistry, Federal University Fluminense, Niterói-RJ 24020-141, Brazil*

Érica de Oliveira Costa − *SupraSelen Laboratory, Department of Organic Chemistry, Institute of Chemistry, Federal University Fluminense, Niterói-RJ 24020-141, Brazil*

Thuany G. Duarte − *SupraSelen Laboratory, Department of Organic Chemistry, Institute of Chemistry, Federal University Fluminense, Niterói-RJ 24020-141, Brazil*

Thiago S. Charret − *Research Laboratory of Natural Products and Bioactive Molecules, Nova Friburgo Health Institute,*

https://doi.org/10.1021/acsomega.3c10134
ACS Omega 2024, 9, 21948−21963

Fluminense Federal University (ISNF-UFF), Nova Friburgo-RJ 28625-650, Brazil

Raquel C. Castiglione − *Laboratory for Clinical and Experimental Research on Vascular Biology, Biomedical Center, State University of Rio de Janeiro, Rio de Janeiro-RJ 20550-900, Brazil*

Rafael L. Simões − *Laboratory of Molecular and Cellular Pharmacology, Roberto Alcântara Gomes Biology Institute, State University of Rio de Janeiro, Rio de Janeiro 20551-030, Brazil*

Vinicius D. B. Pascoal − *Research Laboratory of Natural Products and Bioactive Molecules, Nova Friburgo Health Institute, Fluminense Federal University (ISNF-UFF), Nova Friburgo-RJ 28625-650, Brazil*

Thiago H. Döring − *Department of Exact Sciences and Education, Federal University of Santa Catarina, Blumenau-SC 89036-256, Brazil*

Fernando de C. da Silva − *Applied Organic Synthesis Laboratory (LabSOA), Institute of Chemistry, Universidade Federal Fluminense, Niterói-RJ 24020-141, Brazil;* orcid.org/0000-0002-2042-3778

Vitor F. Ferreira − *Department of Exact Sciences and Education, Federal University of Santa Catarina, Blumenau-SC 89036-256, Brazil*

Aldo S. de Oliveira − *Department of Exact Sciences and Education, Federal University of Santa Catarina, Blumenau-SC 89036-256, Brazil;* orcid.org/0000-0001-7760-4484

Aislan C. R. F. Pascoal − *Research Laboratory of Natural Products and Bioactive Molecules, Nova Friburgo Health Institute, Fluminense Federal University (ISNF-UFF), Nova Friburgo-RJ 28625-650, Brazil*

André L. S. Cruz − *Physiopathology Laboratory, Institute of Medical Sciences, Multidisciplinary Center UFRJ, Federal University of Rio De Janeiro (UFRJ), Macaé-RJ 27930-560, Brazil*

Complete contact information is available at: https://pubs.acs.org/10.1021/acsomega.3c10134

Notes

The authors declare no competing financial interest.

■ ACKNOWLEDGMENTS

We would like to thank the Fundação de Amparo à Pesquisa do Estado do Rio de Janeiro - FAPERJ (E-26/202.911/2019, E-26/200.414/2020, E-26/210.325/2022, and E-26/200.235/2023), the Conselho Nacional de Desenvolvimento Científico e Tecnológico - CNPq (310656/2021-4), the Coordenação de Aperfeiçoamento de Pessoal de Nível Superior - Brazil (CAPES) - Financing Code 001 and INCT-Catálise for the financial support provided.

■ REFERENCES

(1) Yang, Z.; Yan, G.; Zheng, L.; Gu, W.; Liu, F.; Chen, W.; Cui, X.; Wang, Y.; Yang, Y.; Chen, X.; et al. YKT6, as a potential predictor of prognosis and immunotherapy response for oral squamous cell carcinoma, is related to cell invasion, metastasis, and CD8+ T cell infiltration. *Oncoimmunology* **2021**, *10*, No. e1938890.

(2) Wang, Z.; Guan, W.; Ma, Y.; Zhou, X.; Song, G.; Wei, J.; Wang, C. MicroRNA-191 regulates oral squamous cell carcinoma cells growth by targeting PLCD1 via the Wnt/β-catenin signaling pathway. *BMC Cancer* **2023**, *23*, 668.

(3) Ghantous, Y.; Elnaaj, I. A. Global incidence and risk factors of oral cancer. *Harefuah* **2017**, *156*, 645.

(4) Chattopadhyay, A.; Weatherspoon, D.; Pinto, A. Human papillomavirus and oral cancer: a primer for dental public health professionals. *Community Dent. Health* **2015**, *32* (2), 117.

(5) Ali, K. Oral cancer - the fight must go on against all odds. *Evid Based Dent.* **2022**, *23*, 4.

(6) Wang, N.; Huang, M.; Lv, H. Head and neck verrucous carcinoma: A population-based analysis ofincidence, treatment, and prognosis. *Medicine* **2020**, *99*, No. e18660.

(7) Qiao, C. Y.; Qiao, T. Y.; Jin, H.; Liu, L. L.; Zheng, M. D.; Wang, Z. L. LncRNA KCNQ1OT1 contributes to the cisplatin resistance of tongue cancer through the KCNQ1OT1/miR-124−3p/TRIM14 axis. *Eur. Rev. Med. Pharmacol. Sci.* **2020**, *24* (1), 200.

(8) Yıldız, M.; Yıldırım, H.; Bayrak, N.; Çakmak, S. M.; Mataracı-Kara, E.; Özbek-Çelik, B.; Otsuka, M.; Fujita, M. O.; Radwan, M.; TuYuN, A. F. Design, synthesis, in vitro and in silico characterization of plastoquinone analogs containing piperidine moiety as antimicrobial agents. *J. Mol. Struct.* **2023**, *1277*, 134845.

(9) Liu, Z.; Shen, Z.; Xiang, S.; Sun, Y.; Cui, J.; Jia, J. Evaluation of 1,4-naphthoquinone derivatives as antibacterial agents: Activity and mechanistic studies. *Front Environ. Sci. Eng.* **2023**, *17* (3), 31.

(10) Wan, Y.; Wang, X.; Yang, L.; Li, Q.; Zheng, X.; Bai, T.; Wang, X. Antibacterial Activity of Juglone Revealed in a Wound Model of Staphylococcus aureus Infection. *Int. J. Mol. Sci.* **2023**, *24* (4), 3931.

(11) Mujawah, A.; Rauf, A.; Bawazeer, S.; Wadood, A.; Hemeg, H. A.; Bawazeer, S. In-vitro antioxidant, lipoxygenase inhibitory, and in-vivo muscle relaxant potential of the extract and constituent isolated from *Diospyros kaki* (Japanese Persimmon). *Heliyon* **2023**, *9*, No. e13816.

(12) Cabral, R. G.; Viegas, G.; Pacheco, R.; Sousa, A. C.; Robalo, M. P. Sustainable Synthesis, Antiproliferative and Acetylcholinesterase Inhibition of 1,4- and 1,2-Naphthoquinone Derivatives. *Molecules* **2023**, *28*, 1232.

(13) Santos, L. H.; Kronenberger, T.; Almeida, R. G.; Silva, E. B.; Rocha, R. E. O.; Oliveira, J. C.; Barreto, L. V.; Skinner, D.; Fajtová, P.; Giardini, M. A.; et al. Structure-Based Identification of Naphthoquinones and Derivatives as Novel Inhibitors of Main Protease Mpro and Papain-like Protease PLpro of SARS-CoV-2. *J. Chem. Inf. Model.* **2022**, *62*, 6553−6573.

(14) Kumagai, Y.; Shinkai, Y.; Miura, T.; Cho, A. K. The Chemical Biology of Naphthoquinones and Its Environmental Implications. *Rev. Pharmacol. Toxicol.* **2012**, *52*, 221−247.

(15) Pereyra, C. E.; Dantas, R. F.; Ferreira, S. B.; Gomes, L. P.; Silva-Jr, F. P. The diverse mechanisms and anticancer potential of naphthoquinones. *Cancer Cell Int.* **2019**, *19* (1), 207.

(16) Stangel, M.; Zettl, U. K.; Mix, E.; Zielasek, J.; Toyka, K. V.; Hartung, H. P.; Gold, R. H2O2 and nitric oxide-mediated oxidative stress induce apoptosis in rat skeletal muscle myoblasts. *J. Neuropathol. Exp. Neurol.* **1996**, *55*, 36−43.

(17) Abreu, F. C.; Ferraz, p'. A. L.; Goulart, M. O. F. Some Applications of Electrochemistry in Biomedical Chemistry. Emphasis on the Correlation of Electrochemical and Bioactive Properties. *J. Braz. Chem. Soc.* **2002**, *13* (1), 19−35.

(18) López, L. I. L.; Flores, S. D. N.; Belmares, S. Y. S.; Galindo, A. S. Naphthoquinones: biological properties and synthesis of lawsone and derivatives—a structured review. *Vitae* **2014**, *21*, 248−258.

(19) Pereyra, C. E.; Dantas, R. F.; Ferreira, S. B.; Gomes, L. P.; Silva-Jr, F. P. The diverse mechanisms and anticancer potential of naphthoquinones. *Cancer Cell Int.* **2019**, *19* (1), 207.

(20) Alotaibi, J. S.; Al-Faiyz, Y. S.; Shaaban, S. Design, Synthesis, and Biological Evaluation of Novel Hydroxamic Acid-Based Organoselenium Hybrids. *Pharmaceuticals* **2023**, *16* (3), 367.

(21) Zaki, R. M.; Wani, M. Y.; Mohammed, A.; El-Said, W. A. Design, synthesis and evaluation of novel Se-alkylated pyrazoles and their cyclized analogs as potential anticancer agents. *J. Mol. Struct.* **2023**, *1276*, 134670.

(22) Zhong, M.; Lu, Y.; Li, S.; Li, X.; Liu, Z.; He, X.; Zhang, Y. Synthesis, cytotoxicity, antioxidant activity and molecular modeling of new NSAIDs-EBS derivatives. *Eur. J. Med. Chem.* **2023**, *259*, 115662.

(23) Sarturi, J. M.; Dornelles, L.; Segatto, N. V.; Collares, T.; Seixas, F. K.; Piccoli, B. C.; Da Silva, F. D.; Omage, F. B.; Rocha, J. B. T.; Balaguez, R. A.; et al. Chalcogenium-AZT Derivatives: A Plausible Strategy To Tackle The RT-Inhibitors-Related Oxidative Stress While Maintaining Their Anti-HIV Properties. *Curr. Med. Chem.* **2023**, *30* (21), 2449−2462.
(24) Refaay, D. A.; Ahmed, D. M.; Mowafy, A. M.; Shaaban, S. Evaluation of novel multifunctional organoselenium compounds as potential cholinesterase inhibitors against Alzheimer's disease. *Med. Chem. Res.* **2022**, *31*, 894−904.
(25) Gomes, L. S.; Neto, J. S. S.; Di Leo, I.; Barbosa, C. G.; Moraes, C. B.; Freitas-Junior, L. H.; Rizzuti, B.; Santi, C.; Nascimento, V. Ecofriendly aminochalcogenation of alkenes: a green alternative to obtain compounds with potential anti-SARS-CoV-2 activity. *New J. Chem.* **2023**, *47*, 6591−6601.
(26) Gritzenco, F.; Kazmierczak, J. C.; Anjos, T.; Sperança, A.; Peixoto, M. L. B.; Godoi, M.; Ledebuhr, K. N. B.; Brüning, C. A.; Zamin, L. L.; Godoi, B. Base-Free Synthesis and Synthetic Applications of Novel 3-(Organochalcogenyl) prop-2-yn-1-yl Esters: Promising Anticancer Agents. *Synthesis* **2021**, *53*, 2676−2688.
(27) Hu, J.; Chen, L.; Lu, Z.; Yao, H.; Hu, Y.; Feng, L.; Pang, Y.; Wu, J.; Yu, Z.; Chen, W.-H. Design, Synthesis and Antitumor Activity of Novel Selenium-Containing Tepotinib Derivatives as Dual Inhibitors of c-Met and TrxR. *Molecules* **2023**, *28* (3), 1304.
(28) Radomska, D.; Czarnomysy, R.; Szymanowska, A.; Radomski, D.; Domínguez-Álvarez, E.; Bielawska, A.; Bielawski, K. Novel Selenoesters as a Potential Tool in Triple-Negative Breast Cancer Treatment. *Cancers* **2022**, *14*, 4304.
(29) Rocha, D. R.; Mota, K.; Silva, I. M. C. B.; Ferreira, V. F.; Ferreira, S. B.; Silva, F. D. C. Synthesis of fused chromene-1,4-naphthoquinones via ring-closing metathesis and Knoevenagel-electrocyclization under acid catalysis and microwave irradiation. *Tetrahedron* **2014**, *70* (20), 3266−3270.
(30) Reich, H. J.; Cohen, M. L.; Clark, P. S. Reagents for Synthesis of Organoselenium Compounds: Diphenyl Diselenide and Benzeneselenenyl Chloride. *Org. Synth.* **2023**, *59*, 141.
(31) Mosmann, T. Rapid colorimetric assay for cellular growth and survival: application to proliferation and cytotoxicity assays. *J. Immunol. Methods* **1983**, *65*, 55−63.
(32) Zorzanelli, B. C.; De Queiroz, L. N.; Santos, R. M. A.; Menezes, L. M.; Gomes, F. C.; Ferreira, V. F.; Da Silva, F. D.; Robbs, B. K. Potential cytotoxic and selective effect of new benzo[b]xanthenes against oral squamous cell carcinoma. *Future Med. Chem.* **2018**, *10* (10), 1141−1157.
(33) Macedo, A. L.; Da Silva, D. P. D.; Moreira, D. L.; De Queiroz, L. N.; Vasconcelos, T. R. A.; Araujo, G. F.; Kaplan, M. A. C.; Pereira, S. S. C.; De Almeida, S. P.; Valverde, A. L.; et al. Cytotoxicity and selectiveness of Brazilian Piper species towards oral carcinoma cells. *Biomed. Pharmacother.* **2019**, *110*, 342−352.
(34) Hartner, L. Chemotherapy for Oral Cancer. *Dent. Clin. N Am.* **2018**, *62*, 87−97.
(35) Ho, G. Y.; Woodward, N.; Coward, J. I. Cisplatin versus carboplatin: comparative review of therapeutic management in solid malignancies. *Crit. Rev. Oncol. Hematol.* **2016**, *102*, 37−46.
(36) Khasraw, M.; Bell, R.; Dang, C. E. Epirubicin: Is it like doxorubicin in breast cancer? A clinical review. *The Breast* **2012**, *21* (2), 142−149.
(37) Shafei, A.; El-Bakly, W.; Sobhy, A.; Wagdy, O.; Reda, A.; Aboelenin, O.; Marzouk, A.; El Habak, K.; Mostafa, R.; Ali, M. A.; et al. A review on the efficacy and toxicity of different doxorubicin nanoparticles for targeted therapy in metastatic breast cancer. *Biomed. Pharmacother.* **2017**, *95*, 1209−1218.
(38) Hasoon, M. R. A.; Kadhim, N. J. Improvement of the Selectivity Index (SI) and Cytotoxicity Activity of Doxorubicin Drug by Panax ginseng Plant Extract. *Arch. Razi Inst.* **2021**, *76*, 659−666.
(39) Hanahan, D.; Weinberg, R. A. The hallmarks of cancer. *Cell* **2000**, *100*, 57−70.
(40) Hanahan, D.; Weinberg, R. A. Hallmarks of cancer: the next generation. *Cell* **2011**, *144*, 646−674.
(41) Yilmaz, M.; Christofori, G. EMT, the cytoskeleton, and cancer cell invasion. *Cancer Metastasis Rev.* **2009**, *28* (1−2), 15−33.
(42) Martinotti, S.; Ranzato, E. Scratch Wound Healing Assay. *Methods Mol. Biol.* **2019**, *2109*, 225−229.
(43) Mansilla, S.; Llovera, L.; Portugal, J. Chemotherapeutic Targeting of Cell Death Pathways. *Anticancer Agents Med. Chem.* **2012**, *12*, 226−238.
(44) Matthews, H. K.; Bertoli, C.; De Bruin, R. A. M. Cell cycle control in cancer. *Nat. Rev. Mol. Cell Biol.* **2022**, *23*, 74−88.
(45) Pozarowski, P.; Darzynkiewicz, Z. Analysis of cell cycle by flow cytometry. *Methods Mol. Biol.* **2004**, *281*, 301−311.
(46) Thorn, C. F.; Oshiro, C.; Marsh, S.; Hernandez-Boussard, T.; McLeod, H.; Klein, T. E.; Altman, R. B. Doxorubicin pathways: pharmacodynamics and adverse effects. *Pharmacogenet. Genomics* **2011**, *21*, 440−446.
(47) Aminin, D.; Polonik, S. 1,4-Naphthoquinones: Some Biological Properties and Application. *Chem. Pharm. Bull.* **2020**, *68*, 46−57.
(48) Jamier, V.; Ba, L. A.; Jacob, C. Selenium- and tellurium-containing multifunctional redox agents as biochemical redox modulators with selective cytotoxicity. *Chemistry* **2010**, *16*, 10920−10928.
(49) Mecklenburg, S.; Shaaban, S.; Ba, L. A.; Burkholz, T.; Schneider, T.; Diesel, B.; Kiemer, B. A. K.; Röseler, A.; Becker, K.; Reichrath, J.; et al. Exploring synthetic avenues for the effective synthesis of selenium- and tellurium-containing multifunctional redox agents. *Org. Biomol. Chem.* **2009**, *7*, 4753−4762.
(50) Du, P.; Saidu, N. E.; Intemann, J.; Jacob, C.; Montenarh, M. A new tellurium-containing amphiphilic molecule induces apoptosis in HCT116 colon cancer cells. *Biochim. Biophys. Acta* **2014**, *1840*, 1808−1816.
(51) Balducci, L.; Falandry, C.; List, A. A Proactive Approach to Prevent Hematopoietic Exhaustion During Cancer Chemotherapy in Older Patients: Temporary Cell-Cycle Arrest. *Drugs Aging* **2023**, *40*, 263−272.
(52) Rahman, M. M.; Islam, M. R.; Akash, S.; Shohag, S.; Ahmed, L.; Supti, F. A.; Rauf, A.; Aljohani, A. S. M.; Abdulmonem, W. A.; Khalil, A. A.; et al. Naphthoquinones and derivatives as potential anticancer agents: An updated review. *Chem. Biol. Interact.* **2022**, *368*, 110198.
(53) Liu, T.; Xu, L.; He, L.; Zhao, J.; Zhang, Z.; Chen, Q.; Chen, T. Selenium nanoparticles regulates selenoprotein to boost cytokine-induced killer cells-based cancer immunotherapy. *Nano Today* **2020**, *35*, 100975.
(54) Domínguez-Álvarez, E.; Rácz, B.; Marć, M. A.; Nasim, M. J.; Szemerédi, N.; Viktorová, J.; Jacob, C.; Spengler, G. Selenium and tellurium in the development of novel small molecules and nanoparticles as cancer multidrug resistance reversal agents. *Drug Resistance Updates* **2022**, *63*, 100844.
(55) Trindade, C.; Juchem, A. L. M.; Guecheva, T. N.; De Oliveira, I. M.; Silveira, P. S.; Vargas, J. E.; Puga, R.; Pessoa, C. Ó.; Henriques, J. A. P. Diphenyl Ditelluride: Redox-Modulating and Antiproliferative Properties. *Oxid. Med. Cell. Longev* **2019**, *2019*, 1−14.
(56) Tripathi, A.; Khan, A.; Srivastava, R. Synthesis and screening for anticancer activity of two novel telluro-amino acids: 1,3-Tellurazolidine-4-carboxylic acid and tellurohomocystine. *Amino Acids* **2023**, *55* (10), 1361−1370.
(57) Zorzanelli, B. C.; Ouverney, G.; Pauli, F. P.; Da Fonseca, A. C. C.; De Almeida, E. C. P.; De Carvalho, D. G.; Possik, P. A.; Rabelo, V. W.; Abreu, P. A.; Pontes, B.; et al. Pro-Apoptotic Antitumoral Effect of Novel Acridine-Core Naphthoquinone Compounds against Oral Squamous Cell Carcinoma. *Molecules* **2022**, *27*, 5148.
(58) Borges, A. A.; De Souza, M. P.; Da Fonseca, A. C. C.; Wermelinger, G. F.; Ribeiro, R. C. B.; Amaral, A. A. P.; De Carvalho, C. J. C.; Abreu, L. S.; De Queiroz, L. N.; De Almeida, E. C. P.; et al. Chemoselective Synthesis of Mannich Adducts from 1,4-Naphthoquinones and Profile as Autophagic Inducers in Oral Squamous Cell Carcinoma. *Molecules* **2023**, *28*, 309.
(59) Wermelinger, G. F.; Rubini, L.; Da Fonseca, A. C. C.; Ouverney, G.; De Oliveira, R. P. R. F.; De Souza, A. S.; Forezi, L. S. D. M.; Limaverde-Sousa, G.; Pinheiro, S.; Robbs, B. K. A Novel

https://doi.org/10.1021/acsomega.3c10134
ACS Omega 2024, 9, 21948−21963

MDM2-Binding Chalcone Induces Apoptosis of Oral Squamous Cell Carcinoma. *Biomedicines* **2023**, *11*, 1711.
(60) Li, Q.; Sham, H. L.; Rosenberg, S. H. Chapter 14. Antimitotic Agents. *Annu. Rep. Med. Chem.* **1999**, *34*, 139−148.
(61) Elmeliegy, M.; Vourvahis, M.; Guo, C.; Wang, D. D. Effect of P-glycoprotein (P-gp) Inducers on Exposure of P-gp Substrates: Review of Clinical Drug−Drug Interaction Studies. *Clin. Pharmacokinet.* **2020**, *59*, 699−714.
(62) Mollazadeh, S.; Sahebkar, A.; Hadizadeh, F.; Behravan, J.; Arabzadeh, S. Structural and functional aspects of P-glycoprotein and its inhibitors. *Life Sci.* **2018**, *214*, 118−123.
(63) Tripathi, A.; Khan, A.; Srivastava, R. Synthesis and screening for anticancer activity of two novel telluro-amino acids: 1,3-Tellurazolidine-4-carboxylic acid and tellurohomocystine. *Amino Acids* **2023**, *55*, 1361−1370.
(64) Barcellos, A. M.; Abenante, L.; Sarro, M. T.; Leo, I. D.; Lenardao, E. J.; Perin, G.; Santi, C. New Prospective for Redox Modulation Mediated by Organo selenium and Organotellurium Compounds. *Curr. Org. Chem.* **2017**, *21* (20), 2044−2061.
(65) Lipinski, C. A.; Lombardo, F.; Dominy, B. W.; Feeney, P. J. Experimental and computational approaches to estimate solubility and permeability in drug discovery and development settings. *Adv. Drug Delivery Rev.* **2012**, *64*, 4−17.
(66) Cheng, T.; Zhao, Y.; Li, X.; Lin, F.; Xu, Y.; Zhang, X.; Li, Y.; Wang, R.; Lai, L. Computation of octanol-water partition coefficients by guiding an additive model with knowledge. *J. Chem. Inf. Model.* **2007**, *47*, 2140−2148.
(67) Lipinski, C. A.; Lombardo, F.; Dominy, B. W.; Feeney, P. J. Experimental and computational approaches to estimate solubility and permeability in drug discovery and development settings. *Adv. Drug Delivery Rev.* **2001**, *46*, 3−26.
(68) O'Brien, P. J. Molecular mechanisms of quinone cytotoxicity. *Chem. Biol. Interact.* **1991**, *80*, 1−41.
(69) Domínguez-Álvarez, E.; Rácz, B.; Marc, M. A.; Nasim, M. J.; Szemerédi, N.; Viktorová, J.; Jacob, C.; Spengler, G. Selenium and tellurium in the development of novel small molecules and nanoparticles as cancer multidrug resistance reversal agentes. *Drug Resistance Updates* **2022**, *63*, 100844.
(70) Valente, A.; Podolski-Renic, A.; Poetsch, A.; Filipovic, N.; Lopez, O.; Turel, I.; Heffeter, P. Metal- and metalloid-based compounds to target and reverse cancer multidrug resistance. *Drug Resistance Updates* **2021**, *58*, 100778.
(71) Li, W.; Zhang, H.; Assaraf, Y. G.; Zhao, K.; Xu, X.; Xie, J.; Yang, D.; Chen, Z. Overcoming ABC transporter-mediated multidrug resistance: Molecular mechanisms and novel therapeutic drug strategies. *Drug Resistance Updates* **2016**, *27*, 14−29.
(72) Zhitomirsky, B.; Assaraf, Y. G. Lysosomes as mediators of drug resistance in cancer. *Drug Resistance Updates* **2016**, *24*, 23−33.
(73) Su, Z.; Dong, S.; Zhao, S.; Liu, K.; Tan, Y.; Jiang, X.; Assaraf, Y. G.; Qin, B.; Chen, Z.; Zou, C. Novel nanomedicines to overcome cancer multidrug resistance. *Drug Resistance Updates* **2021**, *58*, 100777.
(74) Wang, J. Q.; Yang, Y.; Cai, C. Y.; Teng, Q. X.; Cui, Q.; Lin, J.; Assaraf, Y. G.; Chen, Z. S. Multidrug resistance proteins (MRPs): Structure, function and the overcoming of cancer multidrug resistance. *Drug Resistance Updates* **2021**, *54*, 100743.
(75) Verdonk, M. L.; Chessari, G.; Cole, J. C.; Hartshorn, M. J.; Murray, C. W.; Nissink, J. W. M.; Taylor, R. D.; Taylor, R. Modeling Water Molecules in Protein−Ligand Docking Using GOLD. *J. Med. Chem.* **2005**, *48*, 6504−6515.
(76) Jurrus, E.; Engel, D.; Star, K.; Monson, K.; Brandi, J.; Felberg, L. E.; Brookes, D. H.; Wilson, L.; Chen, J.; Liles, K.; et al. Improvements to the APBS biomolecular solvation software suite. *Protein Sci.* **2018**, *27*, 112−128.
(77) Bank, R. E.; Holst, M. A New Paradigm for Parallel Adaptive Meshing Algorithms. *SIAM Rev.* **2003**, *45*, 291−323.
(78) *ACD/ChemSketch, version 2021.1. 1*, Advanced Chemistry Development Inc, Toronto, ON, Canada, www.acdlabs.com, (accessed 21 07 2021) 2023.
(79) Hanwell, M. D.; Curtis, D. E.; Lonie, D. C.; Vandermeersch, T.; Zurek, E.; Hutchison, G. R. Avogadro: An advanced semantic chemical editor, visualization, and analysis platform. *J. Cheminf.* **2012**, *4* (1), 17.
(80) *ChemAxon. MarvinSketch (version 22.11)*. https://www.chemaxon.com, (accessed 21 07 2022) 2023.
(81) Daina, A.; Michielin, O.; Zoete, V. SwissADME: a free web tool to evaluate pharmacokinetics, drug-likeness and medicinal chemistry friendliness of small molecules. *Sci. Rep.* **2017**, *7* (1), 42717.

https://doi.org/10.1021/acsomega.3c10134
ACS Omega 2024, 9, 21948−21963